Nonlinear Analysis: Hybrid Systems 4 (2010) 451–474

Contents lists available at ScienceDirect

Nonlinear Analysis: Hybrid Systems

journal homepage: www.elsevier.com/locate/nahs

Nonsmooth bifurcations of equilibria in planar continuous systems

J.J. Benjamin Biemond *, Nathan van de Wouw, Henk Nijmeijer

Department of Mechanical Engineering, Eindhoven University of Technology, P.O. Box 513, 5600 MB Eindhoven, The Netherlands

ARTICLE INFO

Article history:
Received 22 September 2009
Accepted 5 November 2009

Keywords:
Nonlinear systems
Bifurcations
Limit cycles
Stability analysis
Hybrid systems
Piecewise linear systems
Local approximation

ABSTRACT

In this paper we present a procedure to find all limit sets near bifurcating equilibria in a class of hybrid systems described by continuous, piecewise smooth differential equations. For this purpose, the dynamics near the bifurcating equilibrium is locally approximated as a piecewise affine systems defined on a conic partition of the plane. To guarantee that all limit sets are identified, conditions for the existence or absence of limit cycles are presented. Combining these results with the study of return maps, a procedure is presented for a local bifurcation analysis of bifurcating equilibria in continuous, piecewise smooth systems. With this procedure, all limit sets that are created or destroyed by the bifurcation are identified in a computationally feasible manner.

1. Introduction

In this paper, local bifurcations are studied for a class of hybrid systems described by continuous, piecewise smooth differential equations. This type of system models can be used to describe mechanical, electrical, biological or economical systems; see e.g. [1–4]. These systems can exhibit the so-called discontinuity-induced bifurcations; see [1,5]. In this paper, we study discontinuity-induced bifurcations of equilibria in planar systems. We present a procedure to find all limit sets, which are created or destroyed by the bifurcation of an equilibrium point. Using this procedure, all these limit sets are identified in a computationally feasible manner.

The state space of piecewise smooth systems can be partitioned in a number of domains where the dynamics is smooth, and their boundaries, where the dynamics is nonsmooth. Discontinuity-induced bifurcations are topological changes in behaviour when system parameters are varied around the values where a limit set collides with such a boundary. Although the effect of such bifurcations is observed both in simulations and experiments, [1,5], no complete theory is available to describe these bifurcations.

In planar autonomous systems, limit sets can be equilibria, periodic orbits (including limit cycles), homoclinic or heteroclinic orbits. Discontinuity-induced bifurcations of periodic orbits and homoclinic or heteroclinic orbits can be studied by taking a Poincaré section transversal to these orbits and analysing the resulting return map. In this manner, bifurcations of limit cycles in piecewise smooth dynamical systems are rather well understood; cf. [5,6].

Several studies exist in which bifurcations of equilibria are investigated, where at the bifurcation point the equilibrium is positioned on a single, smooth boundary; see [5,7,8]. However, no theoretical result is available when this equilibrium is positioned on multiple boundaries, or when the boundary is a locally nonsmooth curve in state space. Existence of such bifurcations was recognized in numerical simulations of exemplary systems in [7,9].

The main contribution of this paper is a procedure for a class of planar hybrid systems, namely systems described by continuous, piecewise smooth differential equations, to find all limit sets that can be created or destroyed during a

* Corresponding author. Tel.: +31 402474092; fax: +31 402461418.
E-mail addresses: j.j.b.biemond@tue.nl (J.J.B. Biemond), n.v.d.wouw@tue.nl (N. van de Wouw), h.nijmeijer@tue.nl (H. Nijmeijer).

1751-570X/$ – see front matter © 2009 Elsevier Ltd. All rights reserved.
doi:10.1016/j.nahs.2009.11.003

bifurcation of an equilibrium. Using this procedure, all limit sets that are created or destroyed during a bifurcation are identified in a computationally feasible manner.

To analyse the dynamics near the bifurcation point, we construct a local approximation of the dynamics in a neighbourhood of the bifurcating equilibrium, such that we obtain an approximate system, where the dynamics is affine with respect to the bifurcation parameter in each smooth domain, that is a cone. Furthermore, the dynamics is dependent on the bifurcation parameter in the affine term. These systems are called conewise affine systems, and also represent a class of hybrid systems. We derive criteria under which the limit set of the nonsmooth systems are accurately described by the approximated system.

To exclude closed orbits in certain regions of state space, the Bendixson Theorem and index theory are used. To obtain all closed orbits in the remaining part of the state space, return maps are derived, whose Poincaré sections are chosen at locations, determined by the investigation of specific trajectories. Fixed points of these return maps determine the existence, location and stability of limit cycles or closed orbits.

We derive general conditions for the existence of a halfline in the conewise affine system, that cannot be traversed by closed orbits. Using these conditions, one can guarantee that all limit sets can be found in a computationally feasible manner with the given procedure. According to index theory, closed orbits, including limit cycles, should encircle at least one equilibrium point. Derivation of all possible return maps for the trajectories that cross a line between the equilibria and the halfline, mentioned above, will obtain all existing closed orbits. The domain of these return maps is bounded, such that all fixed points can be detected efficiently with numerical methods.

Although the Poincaré–Bendixson theorem can be used to give sufficient conditions for the existence of limit cycles, cf. [10], we will use a different approach to guarantee, that all limit cycles are identified.

This paper is organized as follows. In Section 2 some preliminary results are given, including the local approximation of the piecewise smooth system by a conewise affine system. Subsequently, in Section 3 the stability of an equilibrium of the resulting conewise affine system at the bifurcation point is investigated. In Section 4 the main theoretical results of this paper are presented, together with the procedure to find all limit sets near the bifurcation point. Subsequently, in Section 5, the effect of the used approximation is studied. The presented procedure is illustrated with examples in Section 6. Finally, conclusions are formulated in Section 7.

2. Preliminaries

Throughout this paper, for the sake of brevity we will adopt the term *nonsmooth systems* to annotate the class of continuous piecewise smooth systems. These systems can be described by the ordinary differential equation:

$$\begin{aligned} &\dot{\mathbf{x}} = \mathbf{F}(\mathbf{x}, \nu), \\ &\mathbf{F}(\mathbf{x}, \nu) = \mathbf{F}_i(\mathbf{x}, \nu), \quad \mathbf{x} \in \mathcal{D}_i \subset \mathbb{R}^2, \end{aligned} \tag{1}$$

where $\mathcal{D}_i,\ i = 1, \ldots, \bar{m}$, are open, non-overlapping domains such that $\cup_{i\in\{1,\ldots,\bar{m}\}} \bar{\mathcal{D}}_i = \mathbb{R}^2$, all functions $\mathbf{F}_i$ are smooth in $\mathbf{x}$ for all $\mathbf{x} \in \mathbb{R}^2$, and smooth in ν for all $\nu \in \mathbb{R}$, which is a single system parameter. Throughout this paper, let $\bar{\mathcal{D}}$ denote the closure of an open set $\mathcal{D}$. We assume that the domains $\mathcal{D}_i,\ i = 1, \ldots, \bar{m}$, are independent on the system parameter ν. These domains are separated by the boundaries $\mathcal{C}_{ij}$ between $\mathcal{D}_i$ and $\mathcal{D}_j$. Note that the boundaries $\mathcal{C}_{ij}$ can be nonsmooth curves in $\mathbb{R}^2$. Let the domains $\mathcal{D}_i,\ i = 1, \ldots, \bar{m}$, and boundaries $\mathcal{C}_{ij}$ be such that every finite line segment in $\mathbb{R}^2$ traverses each boundary $\mathcal{C}_{ij}$ a finite number of times. Similar to the approach given in [11], one can prove that $\mathbf{F}(\mathbf{x}, \nu)$ is Lipschitz continuous in $\mathbf{x}$.

In this paper, we adopt the following assumptions:

Assumption 1. At $\nu = 0$, a single isolated equilibrium coincides with one or more boundaries $\mathcal{C}_{ij}$.

Without loss of generality, we will assume this equilibrium point is positioned at the origin for $\nu = 0$.

Assumption 2. The derivative $\left.\frac{\partial \mathbf{F}}{\partial \nu}\right|_{(\mathbf{x},\nu)=(\mathbf{0},0)} \neq \mathbf{0}$.

Under these assumptions, a local analysis of the dynamics around the equilibrium is constructed. Here, the origin of the coordinate system is chosen such that the equilibrium for $\nu = 0$ is positioned at the origin. We will make a local approximation of system (1) that accurately represents the existence and stability of equilibria and limit cycles of the original system, as we will show in Section 5. The boundaries on which the equilibrium is positioned are approximated by halflines that coincide at the equilibrium. In this manner, the neighbourhood of the equilibrium can be partitioned by a number of cones $\mathcal{S}_i,\ i = 1, \ldots, m$, separated by these halflines, where $m \leq \bar{m}$. We denote the boundaries such that the boundary between $\mathcal{S}_i$ and $\mathcal{S}_j$ is denoted as Σ_{ij}. Possibly after renumbering the sets $\mathcal{D}_i, i = 1, \ldots, \bar{m}$, each cone $\mathcal{S}_i,\ i = 1, \ldots m$, is a local approximation of the sets $\mathcal{D}_i$. The smooth vector field $\mathbf{F}_i$ in each of the cones $\mathcal{S}_i,\ i = 1, \ldots, m$, can be approximated by a linear differential equation $\dot{\mathbf{x}} = A_i\mathbf{x}$, where $A_i = \left.\frac{\partial \mathbf{F}_i}{\partial \mathbf{x}}\right|_{(\mathbf{x},\nu)=(\mathbf{0},0)}$. When a Taylor approximation is used to approximate

the effect on $\mathbf{F}(\mathbf{x}, \nu)$ of changes in the system parameter ν, an affine term $\nu \left.\frac{\partial \mathbf{F}}{\partial \nu}\right|_{(\mathbf{x},\nu)=(\mathbf{0},0)}$ is obtained, such that the dynamics is approximated by a conewise affine system, described by:

$$\begin{aligned} &\dot{\mathbf{x}} = \mathbf{f}(\mathbf{x}, \mu), \\ &\mathbf{f}(\mathbf{x}, \mu) = \mathbf{f}_i(\mathbf{x}, \mu) := A_i\mathbf{x} + \mu\mathbf{b}, \quad \mathbf{x} \in \mathcal{S}_i, \end{aligned} \tag{2}$$

where all regions $\mathcal{S}_i$, $i = 1, 2, \ldots, m$, are cones coinciding at the origin, and we define $\mu = \nu \left\| \left.\frac{\partial \mathbf{F}}{\partial \nu}\right|_{(\mathbf{x},\nu)=(\mathbf{0},0)} \right\|^{-1}$, such that $\mathbf{b} := \left.\frac{\partial \mathbf{F}}{\partial \mu}\right|_{(\mathbf{x},\mu)=(\mathbf{0},0)}$ satisfies $\|\mathbf{b}\| = 1$. Here, $\|\cdot\|$ denotes the Euclidian norm of a vector. The matrices A_i are such that the function $\mathbf{f}(\mathbf{x}, \mu)$ is continuous. Choose the indices i of the open sets $\mathcal{S}_i$, $i = 1, \ldots, m$, such that the set $\{\mathcal{S}_1, \ldots \mathcal{S}_m\}$ is ordered in counter clockwise direction. Let Σ_{ij} be the boundary between the cones $\mathcal{S}_i$ and $\mathcal{S}_j$ and let $\{\mathbf{t}_{12} \ldots \mathbf{t}_{m-1,m}, \mathbf{t}_{m1}\}$ be the set of distinct unit vectors in $\mathbb{R}^2$ parallel to the boundaries $\Sigma_{12} \ldots \Sigma_{m-1,m}, \Sigma_{m1}$, respectively. Define $\mathbf{t}_{01} := \mathbf{t}_{m1}$ and $\Sigma_{01} := \Sigma_{m1}$, such that each $\mathcal{S}_i$ is bounded by $\Sigma_{i-1,i} = \{\mathbf{x} \in \mathbb{R}^2 | \mathbf{x} = c\mathbf{t}_{i-1,i}, c \in [0, \infty)\}$ and $\Sigma_{i,i+1} = \{\mathbf{x} \in \mathbb{R}^2 | \mathbf{x} = c\mathbf{t}_{i,i+1}, c \in [0, \infty)\}$. With parameter $\mu = 0$, the system is called conewise linear. Note that (2) is a subclass of the systems given in (1), which implies that the conewise affine system satisfies the Lipschitz condition.

In this paper, the following definition of a cone is used, that is an adapted version of the definition given in [12].

Definition 1. Consider a region $\mathcal{S} \subset \mathbb{R}^n$. If $\mathbf{x} \in \mathcal{S}$ implies $c\mathbf{x} \in \mathcal{S}$, $\forall c \in (0, \infty)$ and $\mathcal{S} \setminus \{\mathbf{0}\}$ is connected, then $\mathcal{S}$ is a cone.

Note that when the bifurcating equilibrium is positioned on a single boundary Σ_{ij}, that is nonsmooth at the origin, then the conewise affine system contains one convex cone, and one nonconvex cone. To assess the validity of the approximation, the relation between limit sets of the nonsmooth system (1) and the conewise affine approximation (2) will be discussed in Section 5.

Similar to [13], we define *visible eigenvectors*.

Definition 2. Let $\dot{\mathbf{x}} = A_i\mathbf{x} + \mu\mathbf{b}$ be the dynamics on an open cone $\mathcal{S}_i \subset \mathbb{R}^2$, $i = 1, \ldots, m$. An eigenvector of A_i is *visible* if it lies in $\bar{\mathcal{S}}_i$.

Based on the index theory presented in [14], we can formulate the following theorem.

Theorem 1. *Inside a closed orbit C of the planar dynamical system $\dot{\mathbf{x}} = \mathbf{f}(\mathbf{x})$, where $\mathbf{f} : E \to \mathbb{R}^2$ is a Lipschitz continuous function on E, at least one equilibrium point exists. If all equilibria inside C are hyperbolic nodes, saddles, or foci, then there must be an odd number $2n + 1$ of equilibria, where n is an integer, such that n equilibria are saddles and $n + 1$ equilibria are nodes or foci.*

The proofs of this and subsequent results can be found in Appendix B.

Isolated closed orbits are limit cycles. According to the definition in [15], all closed orbits are limit sets. The following extension of Bendixson's Theorem is used.

Theorem 2 *([16]). Suppose E is a simply connected domain in $\mathbb{R}^2$ and $\mathbf{f}(\mathbf{x})$ is a Lipschitz continuous vector field on E, such that the quantity $\nabla\mathbf{f}(\mathbf{x}) := \frac{\partial f_1}{\partial x_1}(\mathbf{x}) + \frac{\partial f_2}{\partial x_2}(\mathbf{x})$ is not zero almost everywhere over any subregion of E and is of the same sign almost everywhere in E. Then E does not contain closed trajectories of $\dot{\mathbf{x}} = \mathbf{f}(\mathbf{x})$, where $\mathbf{x} = \begin{pmatrix} x_1 \\ x_2 \end{pmatrix}$ and $\mathbf{f} = \begin{pmatrix} f_1 \\ f_2 \end{pmatrix}$.*

3. Stability of an equilibrium at the bifurcation point

For $\mu = 0$, the dynamics of the system (2) is described by the continuous, conewise linear system:

$$\begin{aligned} &\dot{\mathbf{y}} = \mathbf{f}(\mathbf{y}), \\ &\mathbf{f}(\mathbf{y}) = A_i\mathbf{y}, \quad \mathbf{y} \in \mathcal{S}_i, \ i = 1, \ldots, m. \end{aligned} \tag{3}$$

To analyse the dynamics of the conewise affine system (2), the stability of the equilibrium $\mathbf{y} = \mathbf{0}$ of the conewise linear system (3) is important. The stability result presented here provides necessary and sufficient conditions for the stability of the origin of (3) and is an extension of a result presented in [13], since in that work all cones are required to be convex. For the sake of brevity, in this paper, we restrict ourselves to the case of systems described with differential equations with continuous right-hand side. We note that the stability result presented here can readily be extended to obtain necessary and sufficient conditions for *exponential* stability or to allow for discontinuous functions $\mathbf{f}(\cdot)$ in (3). Here, we refrain from treating such extensions since the focus of the current paper is on bifurcation analysis.

To assess the stability of the equilibrium point $\mathbf{y} = \mathbf{0}$ of (3), we distinguish systems with, or without, visible eigenvectors, as defined in Definition 2. In Section 3.1, the case of systems with visible eigenvectors is discussed. Subsequently in Section 3.2, the case of systems without visible eigenvectors is studied. Finally, in Section 3.3, necessary and sufficient conditions for asymptotic stability of (3) are derived.

3.1. Systems with visible eigenvectors

Here, conewise linear systems of the form (3) with visible eigenvectors are studied. When a closed cone $\bar{\mathcal{S}}$ does contain a visible eigenvector, the following result holds for trajectories inside this cone.

Lemma 3. *Let $\bar{\mathcal{S}}$ be a closed cone, in which the dynamics is described by $\dot{\mathbf{y}} = A\mathbf{y}$, and let there exist a visible eigenvector $\mathbf{v}$ in $\bar{\mathcal{S}}$, corresponding to the eigenvalue $\lambda < 0$. Suppose no visible eigenvectors exist in this cone, associated with $\lambda \geq 0$. Then, all trajectories inside $\bar{\mathcal{S}}$ converge to $\mathbf{y} = \mathbf{0}$ or leave $\bar{\mathcal{S}}$ in finite time.*

A similar result is obtained for trajectories inside cones, that do not contain visible eigenvectors.

Lemma 4. *Let $\bar{\mathcal{S}}$ be a closed cone in $\mathbb{R}^2$. Suppose no eigenvectors of $A \in \mathbb{R}^{2\times 2}$ are visible in $\bar{\mathcal{S}}$. Then for any initial condition $\mathbf{y}_0 \in \bar{\mathcal{S}}$, with $\mathbf{y}_0 \neq \mathbf{0}$, there exists a time $t \geq 0$ such that $\mathrm{e}^{At}\mathbf{y}_0 \notin \bar{\mathcal{S}}$.*

Using the foregoing lemmas, the following result is proven, providing necessary and sufficient conditions for asymptotic stability of the origin of conewise linear systems (3) with visible eigenvectors.

Lemma 5. *Consider a continuous, conewise linear system described by (3). When this system contains one or more cones with visible eigenvectors, then $\mathbf{y} = \mathbf{0}$ is an asymptotically stable equilibrium of (3) if and only if all visible eigenvectors correspond to eigenvalues $\lambda < 0$.*

3.2. Systems without visible eigenvectors

In conewise linear systems (3) without visible eigenvectors, trajectories exhibit a spiralling motion around the origin, visiting each region $\mathcal{S}_i$, $i = 1, \ldots, m$, once per rotation. Stability results are obtained for the spiralling motion by the computation of a return map.

In the absence of visible eigenvectors, a trajectory in the region $\mathcal{S}_i$, $i = 1, \ldots, m$, will traverse this region in finite time. The position $\mathbf{y}_0$ where a trajectory enters this region at time $t_0 = 0$ is located on the boundary $\Sigma_{i-1,i}$, such that $\mathbf{y}_0$ can be expressed as $\mathbf{y}_0 = p^i\mathbf{t}_{i-1,i}$. Furthermore, this trajectory will cross $\Sigma_{i,i+1}$ in a finite time t_i. The position of this crossing can be given as: $\mathbf{y}(t_i) = p^{i+1}\mathbf{t}_{i,i+1}$. Since the dynamics inside the cone are linear, the time t_i can be solved for, such that $\mathbf{y}(t_i)$ is parallel to $\mathbf{t}_{i,i+1}$. In this manner, in [13], expressions for the traversal time and crossing positions are derived. The crossing positions are linear in p^i. Using such analysis, we can derive expressions for a scalar M_i, such that $p^{i+1} = M_i p^i$. Note that similar expressions have been derived in [13] for systems (3) with cones, that are convex.

First, the position vectors $\mathbf{y}$ and tangency vectors $\mathbf{t}$ are represented in a new coordinate frame:

$$\tilde{\mathbf{y}}^i = P_i^{-1}\mathbf{y}, \quad \text{for } \tilde{\mathbf{y}}^i \in \tilde{\mathcal{S}}_i := \{\tilde{\mathbf{y}}^i \in \mathbb{R}^2 | \tilde{\mathbf{y}}^i = P_i^{-1}\mathbf{y},\ \mathbf{y} \in \bar{\mathcal{S}}_i\}, \tag{4}$$

where P_i is given by the real Jordan decomposition of A_i, yielding $A_i = P_i J_i P_i^{-1}$. This decomposition distinguishes three cases.

Case 1: If A_i has complex eigenvalues, then $J_i = \begin{bmatrix} a_i & -\omega_i \\ \omega_i & a_i \end{bmatrix}$, where a_i and ω_i are real constants and $\omega_i > 0$. Define $\Theta(\mathbf{a}_1, \mathbf{a}_2)$ to be the angle in counter clockwise direction from vector $\mathbf{a}_1$ to vector $\mathbf{a}_2$. Herewith,

$$M_i = \frac{\|\tilde{\mathbf{t}}^i_{i-1,i}\|}{\|\tilde{\mathbf{t}}^i_{i,i+1}\|}\mathrm{e}^{\frac{a_i}{\omega_i}\Theta(\tilde{\mathbf{t}}^i_{i-1,i}, \tilde{\mathbf{t}}^i_{i,i+1})}. \tag{5}$$

Case 2: If A_i has two distinct real eigenvalues λ_{ai} and λ_{bi} and two distinct eigenvectors, then $J_i = \begin{bmatrix} \lambda_{ai} & 0 \\ 0 & \lambda_{bi} \end{bmatrix}$ and

$$M_i = \left|\frac{\mathbf{e}_2^T\tilde{\mathbf{t}}^i_{i,i+1}}{\mathbf{e}_2^T\tilde{\mathbf{t}}^i_{i-1,i}}\right|^{\frac{\lambda_{ai}}{\lambda_{bi}-\lambda_{ai}}} \left|\frac{\mathbf{e}_1^T\tilde{\mathbf{t}}^i_{i,i+1}}{\mathbf{e}_1^T\tilde{\mathbf{t}}^i_{i-1,i}}\right|^{\frac{\lambda_{bi}}{\lambda_{ai}-\lambda_{bi}}}, \tag{6}$$

where $\mathbf{e}_1 := \begin{pmatrix} 1 & 0 \end{pmatrix}^T$ and $\mathbf{e}_2 := \begin{pmatrix} 0 & 1 \end{pmatrix}^T$.

Case 3: If A_i has two equal real eigenvalues λ_{ai} with geometric multiplicity 1, then $J_i = \begin{bmatrix} \lambda_{ai} & 1 \\ 0 & \lambda_{ai} \end{bmatrix}$ and

$$M_i = \left|\frac{\mathbf{e}_2^T\tilde{\mathbf{t}}^i_{i-1,i}}{\mathbf{e}_2^T\tilde{\mathbf{t}}^i_{i,i+1}}\right| \mathrm{e}^{\lambda_{ai}\left(\frac{\mathbf{e}_1^T\tilde{\mathbf{t}}^i_{i,i+1}}{\mathbf{e}_2^T\tilde{\mathbf{t}}^i_{i,i+1}} - \frac{\mathbf{e}_1^T\tilde{\mathbf{t}}^i_{i-1,i}}{\mathbf{e}_2^T\tilde{\mathbf{t}}^i_{i-1,i}}\right)}. \tag{7}$$

By computation of the scalars M_i with (5), (6) or (7) for each cone $\mathcal{S}_i$, $i = 1, \ldots, m$, one can compute the return map between the positions $\mathbf{y}_k$ and $\mathbf{y}_{k+1}$ of two subsequent crossings of the trajectory $\mathbf{y}(t)$ with the boundary Σ_{m1}:

$$\mathbf{y}_{k+1} = \Lambda\mathbf{y}_k, \tag{8}$$

where

$$\Lambda = \prod_{i=1}^{m} M_i. \tag{9}$$

3.3. Stability result

Using the results given in Sections 3.1 and 3.2, we can derive necessary and sufficient conditions for the stability of the origin of the conewise linear system (3).

Theorem 6. *The origin of the continuous, conewise linear system (3) is globally asymptotically stable if and only if*

(i) *in each cone* $\mathcal{S}_i,\ i = 1, \ldots, m$, *all visible eigenvectors are associated with eigenvalues* $\lambda < 0$,
(ii) *in case no visible eigenvectors exist, it holds that* $\Lambda < 1$, *with* Λ *defined in (5), (6), (7) and (9).*

4. Bifurcation analysis of a conewise affine system

The limit sets that can occur in planar continuous systems are equilibria, closed orbits and homoclinic or heteroclinic orbits. To analyse the occurring bifurcations in (2), we are interested in characterisation of these limit sets, including their local stability, for different values of the system parameter μ. The relationship between these limit sets and the limit sets of (1) will be discussed in Section 5. The following assumption is adopted to study the conewise affine system (2).

Assumption 3. All matrices $A_i,\ i = 1, \ldots m$, of (2) are invertible.

Note that this assumption implies that for given bifurcation parameter μ, system (2) can exhibit only isolated equilibrium points $\mathbf{x}_{eq}(\mu)$ that satisfy $\mathbf{f}(\mathbf{x}_{eq}(\mu), \mu) = \mathbf{0}$. Solutions of conewise affine systems as given in (2) scale linearly with the bifurcation parameter μ, as formalised in the following lemma.

Lemma 7. *Consider two continuous conewise affine systems* $\dot{\mathbf{x}} = \mathbf{f}(\mathbf{x}) + \mu_i \mathbf{b},\ \mu_i \in (0, \infty),\ i = 1, 2$, *where* $\mathbf{f}(\cdot)$ *is piecewise linear with cone-shaped regions. If* $\phi_1(t)$ *is a solution of* $\dot{\mathbf{x}} = \mathbf{f}(\mathbf{x}) + \mu_1 \mathbf{b}$, *then* $\phi_2(t) = \frac{\mu_2}{\mu_1}\phi_1(t)$ *is a solution of* $\dot{\mathbf{x}} = \mathbf{f}(\mathbf{x}) + \mu_2 \mathbf{b}$.

From this lemma, we conclude that a complete bifurcation diagram can be obtained by finding all existing limit sets at an arbitrary negative, and an arbitrary positive parameter μ, and at the bifurcation point with $\mu = 0$. Subsequently, with Lemma 7, the limit sets for all parameters μ can be found. The conewise affine system (2) is conewise linear if $\mu = 0$. The dynamical behaviour of (2) at $\mu = 0$ is analysed in the previous section.

In continuous, conewise affine systems with $\mu \neq 0$, the trajectories are tangent to a specific boundary Σ_{ij} at zero, one, or all points on this boundary. When at a boundary an isolated point exists, where the trajectories are tangent to the boundary, such a point will be called a *tangency point* and denoted with $\mathcal{T}_{ij}$. We determine all tangency points of the conewise affine system and compute trajectories in forward and backward time through these tangency points and through the origin. When the vector $\mathbf{f}(\mathbf{x}, \mu)$ of (2) is parallel to a boundary at all points of this boundary, then a trajectory exists, that is parallel to the boundary.

In addition, when a node or saddle point exists, the stable and unstable manifold of this point are computed. Computation of this finite number of trajectories yields insight in the possible behaviour of all trajectories. With these manifolds and trajectories, for each domain $\mathcal{S}_i,\ i = 1, \ldots, m$, we can identify which subsets of $\mathcal{S}_i$ contain trajectories that leave or enter this domain and through which boundary. Therewith, one can identify what sequence of boundaries and cones can possibly be visited by closed orbits.

For each of these sequences, a return map is derived. Hence, finding fixed points in these maps is equivalent to finding closed orbits of (2). However, the domain of these maps may be unbounded, such that no feasible computational approach would exist to find all fixed points in the map. Below, we present two theorems, that can be used to find a halfline in state space, that cannot be traversed by any closed orbit. Existence of such a halfline reduces the domain of the map in which fixed points may exist to a bounded domain.

Theorem 8. *Consider the continuous, conewise affine system (2) with constant* $\mu \neq 0$. *Suppose the system does not contain visible eigenvectors. Construct a system*

$$\begin{aligned} &\dot{\mathbf{y}} = \mathbf{f}(\mathbf{y}), \\ &\mathbf{f}(\mathbf{y}) = A_i \mathbf{y}, \quad \mathbf{y} \in \mathcal{S}_i,\ i = 1, \ldots, m, \end{aligned} \tag{10}$$

by setting $\mu = 0$ *in (2). Let* Λ *for this system be defined in (5), (6), (7) and (9). When* $\Lambda \neq 1$, *there exists an* $\mathbf{x}_F \in \Sigma_{m1} \setminus \{\mathbf{0}\}$, *such that all points in the halfline* $R := \{\mathbf{x} \in \Sigma_{m1} |\ \|\mathbf{x}\| \geq \|\mathbf{x}_F\|\}$ *are not part of a closed orbit of (2).*

A similar result is formulated for systems with visible eigenvectors.

Theorem 9. *Consider system (2), satisfying Assumption 3. If visible eigenvectors exist and all boundaries* Σ_{ij} *do not contain a visible eigenvector of* A_i *or* A_j, *then there exists a halfline* $H \subset \mathbb{R}^2$, *such that closed orbits cannot contain a point* $\mathbf{x}_0 \in H$.

When analysing systems described by (2), Theorems 1, 2, 8 and 9 can be exploited to exclude closed orbits in specific regions of state space. However, in certain cases the existence of closed orbits, including limit cycles, cannot be excluded in some parts of the domain $\mathbb{R}^2$.

To find all closed orbits, return maps are constructed for all possible sequences of cones and boundaries. A logical choice for the Poincaré section, on which the return maps are defined, are the positions where trajectories cross a certain boundary. This is possible for all closed orbits that traverse multiple cones. Closed orbits in a single cone encircle a center, since the dynamics in that cone is affine. In the following section, partial maps are constructed. A partial map describes the position of a trajectory before and after the visit of a specific cone $\mathcal{S}_i,\ i = 1, \ldots, m$. Subsequently, we discuss how to combine these partial maps to obtain the return map.

4.1. Trajectories visiting a cone $\mathcal{S}_i$

In the derivation of Theorem 6, a trajectory of a conewise linear system is followed inside a specific cone $\mathcal{S}_i$ during the traversal of this cone. Since the trajectory during this traversal is described by the linear differential equation $\dot{\mathbf{y}} = A_i\mathbf{y}$, an analytical expression for the trajectory $\mathbf{y}(t)$ with initial position $\mathbf{y}_0 \in \Sigma_{i-1,i}$ is derived. With this expression, the traversal time t_i and final position $\mathbf{y}(t_i)$ are obtained. Here, a similar approach is used for the conewise affine system (2).

For a given cone $\mathcal{S}_i,\ i = 1, \ldots, m$, and given boundaries, where the trajectory enters or leaves this domain, the partial map is constructed that gives the exit position as a function of the position, where $\mathcal{S}_i$ is entered. Since (2) is autonomous, we can assume without loss of generality that the domain $\mathcal{S}_i$ is entered at the time $t = 0$. We study a trajectory traversing $\mathcal{S}_i$ from the boundary Σ_- towards the boundary Σ_+ in a finite time t_i. Therefore, the trajectory $\mathbf{x}(t)$ satisfies $\mathbf{x}(t) \in \mathcal{S}_i,\ t \in (0, t_i)$, $\mathbf{x}(0) \in \Sigma_-$ and $\mathbf{x}(t_i) \in \Sigma_+$. We define the maps $\mathbf{g}_i : D_i \subset \Sigma_- \to I_i \subset \Sigma_+$, describing the position $\mathbf{x}(t_i)$ as a function of $\mathbf{x}(0)$. Expressions for $\mathbf{g}_i$ are derived in Appendix A.

4.2. Construction of the return map

The stable or unstable manifolds of nodes and saddle points and the trajectories through tangency points and the origin are computed. Therewith, for each domain $\mathcal{S}_i$, we can identify what subsets of $\mathcal{S}_i$ contain trajectories that leave or enter this domain and through which boundary. Combining these domains, one can identify what sequences of boundaries and cones can contain closed orbits. A return map is computed for each sequence to find all closed orbits and their stability properties.

For example, suppose we want to study whether there exist one or more closed orbits that traverse the regions and boundaries $\mathcal{S}_1, \Sigma_{12}, \mathcal{S}_2, \Sigma_{23}, \mathcal{S}_3, \Sigma_{31}$ in this order. A Poincaré section is taken at the moments where trajectories cross Σ_{31}, the corresponding return map is denoted as $M : D_M \subset \Sigma_{31} \to I_M \subset \Sigma_{31}$. Therewith, $M(\mathbf{x}_k)$ describes the first crossing of a trajectory $\mathbf{x}(t),\ t > 0$ with boundary Σ_{31}, where $\mathbf{x}(t)$ corresponds to the initial condition $\mathbf{x}(0) = \mathbf{x}_k \in D_M$. Define $\mathbf{g}_1 : D_1 \subset \Sigma_{31} \to I_1 \subset \Sigma_{12}$, which can be computed with Appendix A, where $\Sigma_- = \Sigma_{31}$ and $\Sigma_+ = \Sigma_{12}$. In addition, define $\mathbf{g}_2 : D_2 \subset \Sigma_{12} \to I_2 \subset \Sigma_{23}$ and $\mathbf{g}_3 : D_3 \subset \Sigma_{23} \to I_3 \subset \Sigma_{31}$ in a similar fashion. From a combination of $\mathbf{g}_1$, $\mathbf{g}_2$ and $\mathbf{g}_3$, one obtains the return map $M(\mathbf{x}_k) = \mathbf{g}_3 \circ \mathbf{g}_2 \circ \mathbf{g}_1(\mathbf{x}_k)$.

Since M is a return map, every fixed point of this map is on a closed orbit. When this fixed point is isolated, than the periodic orbit is a limit cycle. Furthermore, each closed orbit of (2), that traverses the boundaries and regions in the sequence $\mathcal{S}_1, \Sigma_{12}, \mathcal{S}_2, \Sigma_{23}, \mathcal{S}_3, \Sigma_{31}$, yields a fixed point in M.

The return map M can be computed for the possible sequences of cones and boundaries. By determining the fixed points of such maps, the existence or absence of limit cycles and closed orbits can be investigated. Each return map is continuous, since (2) is Lipschitz continuous, and trajectories of this class of systems are continuous with respect to initial conditions; see [17], Theorem 3.4. Furthermore, the Euclidean norm of the map, $\|M(\mathbf{x})\|$, is monotonously increasing in $\|\mathbf{x}\|$. Monotonicity follows from the fact that the time-reversed system of (2) is Lipschitz as well, such that the inverse of M should exist and should be unique. The norm $\|M(\mathbf{x})\|$ has to be increasing in $\|\mathbf{x}\|$. Otherwise, there exist points $\mathbf{x}_a,\ \mathbf{x}_b \in D_M$, where $\|\mathbf{x}_a\| < \|\mathbf{x}_b\|$ and $\|M(\mathbf{x}_a)\| > \|M(\mathbf{x}_b)\|$. Note that M is a return map, such that there exists a trajectory from $\mathbf{x}_a$ to $M(\mathbf{x}_a)$ and a trajectory from $\mathbf{x}_b$ towards $M(\mathbf{x}_b)$. The positions $\mathbf{x}_a$, $M(\mathbf{x}_a)$, $\mathbf{x}_b$ and $M(\mathbf{x}_b)$ should all be positioned on the same boundary, that is a halfline. If $\|\mathbf{x}_a\| < \|\mathbf{x}_b\|$ and $\|M(\mathbf{x}_a)\| > \|M(\mathbf{x}_b)\|$, in planar systems, the trajectories from $\mathbf{x}_a$ and $\mathbf{x}_b$ have to cross each other before they return to the Poincaré section. Such a crossing is not possible in systems that are Lipschitz. The fact that the return map is continuous and monotonously increasing can be used in the computational approach to find all fixed points.

4.3. Procedure to obtain all closed orbits

In this section, a stepwise procedure is developed, such that all limit sets of (2) are found for negative, positive and zero bifurcation parameter μ. With this procedure, the bifurcations of the continuous, conewise affine system (2) can be described entirely.

Lemma 7 implies, that only an arbitrary positive and negative μ, and $\mu = 0$, should be studied to obtain the *full bifurcation diagram*. Theorems 1 and 2 are used to exclude the existence of closed orbits. For systems without visible eigenvectors, Theorem 8 supplies a bound to exclude closed orbits far away from the origin. If visible eigenvectors exist, Theorem 9 can be applied to bound the domain, in which closed orbits can occur. When Theorem 8 or 9 can be applied, a bounded domain for

the return map remains, such that it is computationally feasible to find all fixed points of the return map with a numerical method. When certain sequences of boundaries and cones may contain closed orbits, return maps will be constructed.

The following procedure yields a bifurcation diagram of (2) that contains all limit sets.

1. Identify all equilibria for positive and negative μ, i.e. the points $\mathbf{x} \in \mathbb{R}^2$ where $\mathbf{f}(\mathbf{x}, \mu) = \mathbf{0}$, with $\mathbf{f}(\mathbf{x}, \mu)$ given in (2).
2. Study the stability of the equilibrium point $\mathbf{x} = \mathbf{0}$ at $\mu = 0$ using Theorem 6. Identify all visible eigenvectors of A_i, $i = 1, \ldots, m$.
3. For both an arbitrary fixed $\mu < 0$ and $\mu > 0$:
   (a) Compute points where the vector field is tangent to the boundaries. Subsequently, compute trajectories through these tangency points and through the origin for a finite time. In addition, compute the eigenvalues of the matrices A_i, $i = 1, \ldots, m$, when an equilibrium exists inside the corresponding cone $\mathcal{S}_i$. When an equilibrium with real eigenvalues exist, compute the stable and unstable manifolds by simulating a trajectory emanating from or converging to this equilibrium in the direction of the eigenvectors. To check whether homoclinic or heteroclinic orbits exist, investigate whether stable and unstable manifolds coincide.
   (b) Identify, if possible, certain domains that cannot contain closed orbits. First, identify the value of $\mathrm{tr}(A_i)$, $i = 1, \ldots, m$ for each region $\mathcal{S}_i$, i.e. the trace of the matrices A_i. According to Theorem 2, a closed orbit should visit regions $\mathcal{S}_i$ where the traces $\mathrm{tr}(A_i)$ have opposite sign or are zero, since $\nabla \mathbf{f}(\mathbf{x}) = \mathrm{tr}(A_i)$ for $\mathbf{x} \in \mathcal{S}_i$.
   Second, identify the character of the existing equilibria. With Theorem 1 one can guarantee that no closed orbits exist in specific domains. For example, according to this theorem, no closed orbits are possible that encircle one hyperbolic saddle and one focus. Subsequently, determine which equilibria should be encircled by possibly existing closed orbits. Finally, when an unbounded domain remains that may contain closed orbits, identify halflines R or H as defined in Theorem 8 or 9. Such halflines will reduce the domain, in which closed orbits can occur, to a bounded domain. Investigate the sequences of cones and boundaries that may be traversed by closed orbits. For these sequences of cones and boundaries, a return map will be constructed.
   (c) Compute the maps $\mathbf{g}_i : \Sigma_{-,i} \to \Sigma_{+,i}$ of the individual cones $\mathcal{S}_i$ that may be traversed by a closed orbit from $\Sigma_{-,i}$ towards $\Sigma_{+,i}$. The derivation of these maps is given in Appendix A. Combination of the maps yields the return maps for the possible sequences of cones and boundaries. Note that when a halfline R or H, as defined in Theorem 8 or 9, respectively, is found that cannot be crossed by a closed orbit, the domains of these maps where fixed points may exist will be bounded. Determine the fixed points of all possible return maps in a numerical manner. Compute the local derivative of the return map at this fixed point, since this determines the stability of the limit cycle or closed orbit.
4. Identify what limit sets appear, disappear or change their local stability for changing μ. Application of Lemma 7 with respect to the limit sets for a given $\mu < 0$ or $\mu > 0$ yields all limit sets for $\mu \neq 0$. Combination with the piecewise linear stability result gives a bifurcation diagram, containing all changes in limit sets and their stability.

The procedure given above yields all changes in the limit sets of the system. Completeness of the obtained limit cycles follows from the fact that for each conewise affine system (2), a finite number of return maps can be determined, that may contain fixed points. Computation of each of these return maps yields all limit cycles.

5. Approximation effects

In this section, the effect of the conewise affine approximation of a nonsmooth system is studied, as introduced in Section 2. Results are presented for the existence and stability of equilibria (Theorem 10) and limit cycles (Theorem 11) in the nonsmooth system (1) when such limit sets exist in the conewise affine system (2) and vise versa. With these theorems, we show the applicability of the procedure for the bifurcation analysis as presented in Section 4 for nonsmooth systems of the form (1).

We will use the following assumptions in addition to Assumptions 1 and 2:

Assumption 4. For all functions $\mathbf{F}_i(\mathbf{x}, \nu)$, $i = 1, \ldots, \bar{m}$, the Jacobian at the origin, i.e. $\left.\frac{\partial \mathbf{F}_i}{\partial \mathbf{x}}\right|_{(\mathbf{x},\nu)=(\mathbf{0},0)}$, is invertible.

Note that this assumption is stricter than Assumption 3, in which only the vector fields $\mathbf{F}_i(\mathbf{x}, \nu)$, $i = 1, \ldots, m$, are considered. In a neighbourhood around the origin, Assumption 4 excludes the existence of non-isolated equilibria in domains $\mathcal{D}_i$ that are cusp-shaped at the origin.

Assumption 5. The equilibria of the nonlinear system (1) do not move locally tangential to the boundaries when ν is varied around 0.

We illustrate Assumption 5 in Fig. 1. This assumption implies $\mathbf{n}_{i-1,i}^T A_i^{-1} \mathbf{b} \neq 0$, $\forall i \in \{1, \ldots, m\}$.

Remark 1. Paths of equilibria that approach the origin through a cusp-shaped region are excluded by Assumption 5.

Without loss of generality, we may assume that $\left\| \left.\frac{\partial \mathbf{F}}{\partial \nu}\right|_{(\mathbf{x},\nu)=(\mathbf{0},0)} \right\| = 1$, yielding $\mu = \nu$. In the following assumption, the occurrence of center-like behaviour is excluded.

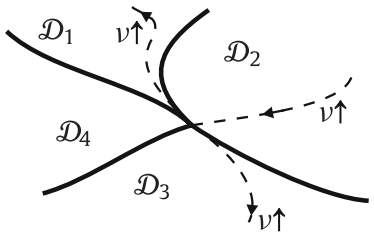

Fig. 1. Paths of equilibria of (1), depicted with dashed lines, where boundaries $\mathcal{C}_{ij}$ are depicted with solid lines. Assumption 5 excludes equilibria emanating tangentially to a boundary, for example the equilibrium path in $\mathcal{D}_3$. In addition, the same assumption excludes equilibria that emanate in a cusp-shaped domain, as depicted in domain $\mathcal{D}_1$.

Assumption 6. In a neighbourhood around the origin, the nonsmooth system (1) and conewise affine system (2) at the bifurcation point $\nu = 0$ or $\mu = 0$ do not contain trajectories that are encircling the equilibrium without converging to the origin for $t \to \infty$ or $t \to -\infty$.

For the conewise affine system, this assumption corresponds to $\Lambda \neq 1$, with Λ given in (9). The following result for the existence of equilibria and the local stability of these equilibria is obtained.

Theorem 10. *Let Assumptions 1, 2, 4 and 5 be satisfied. There exists a neighbourhood $N \subset \mathbb{R}$ of 0, such that for every equilibrium of the nonlinear system (1) that exists for some $\nu \in N$ and converges to the origin for $\nu \to 0$, there exists an equilibrium in the conewise affine system (2). Moreover, for every equilibrium of (2) there will exist an equilibrium in the full nonlinear system for $\nu \in N$.*

When in addition to these assumptions for a given $\nu \in \bar{N}$, with a neighbourhood $\bar{N} \subseteq N$ of 0 chosen small enough, an equilibrium of (1) exists in $\mathcal{D}_i$ or at the origin and the following three conditions hold:

(i) *when the equilibrium of (1) exists in $\mathcal{D}_i$, then the eigenvalues of the corresponding matrix A_i have nonzero real part, and*
(ii) *when this equilibrium has an unstable and stable manifold, no homoclinic or heteroclinic orbit connected to this equilibrium point exist, and*
(iii) *Assumption 6 holds,*

then for every $\nu \in \bar{N}$ the stability properties of the equilibrium of system (1) in $\mathcal{D}_i$ or at the origin and the equilibrium of (2) in $\mathcal{S}_i$ or at the origin, with $\mu = \nu$, are equal.

Remark 2. The combination of Assumption 6 and condition (i) of Theorem 10 for the nonsmooth system (1) can be seen as a counterpart for the assumption of hyperbolic dynamics near equilibria of smooth systems, as would be required to apply the Hartman–Grobman Theorem; cf. [10].

In this work, we will consider limit cycles to be *stable* when, on both sides of the limit cycle, trajectories are converging to the limit cycle. We will refer to limit cycles as *unstable* when, on both sides of the limit cycle, trajectories are diverging from the limit cycle. Limit cycles that are attracting from one side and repelling from the other side are *semi-stable*; cf. [18]. Note that semi-stable limit cycles are unstable in the sense of Lyapunov.

We introduce the following assumptions on the closed orbits of (1) and (2):

Assumption 7. For every closed orbit of (1) and for every closed orbit of (2), a Poincaré map taken transversal to this closed orbit only has isolated fixed points.

Note that this assumption implies that all closed orbits are limit cycles. However, they are allowed to be nonhyperbolic. To state a result on the existence of limit cycles, we need the following restriction on the growth rate of limit cycles when the bifurcation parameter is perturbed:

Assumption 8. For all limit cycles, denoted with γ, of the nonsmooth system (1) there exists a parameter range $\nu \in (0, \nu^*)$ with $\nu^* > 0$ (or $\nu \in (\nu^*, 0)$ with $\nu^* < 0$) and constants $c_1, c_2 > 0$ such that $\|\mathbf{x}\| > c_1|\nu| \wedge \|\mathbf{x}\| < c_2|\nu|, \ \forall \mathbf{x} \in \gamma$ holds for $\nu \in (0, \nu^*)$ (or $\nu \in (\nu^*, 0)$).

This assumption implies that the curve in the bifurcation diagram, depicting the "amplitude" of a limit cycle, has a nonzero finite derivative with respect to the parameter μ at the bifurcation point; cf. Fig. 2. For example, limit cycles γ that show a square-root dependency with respect to the bifurcation parameter ($\|\gamma\| \sim \sqrt{\nu}$) are excluded; such behaviour occurs for example in the Hopf bifurcations of smooth systems.

The following theorem describes the relationship between limit cycles of (1) and (2).

Theorem 11. *Let Assumptions 1, 2, 7 and 8 be satisfied. There exists a neighbourhood N of 0, such that the number of limit cycles in the nonsmooth system (1) for $\nu \in N$ that are not semi-stable, is equal to the number of limit cycles in the approximation (2), which are not semi-stable. In addition, their stability properties are equal.*

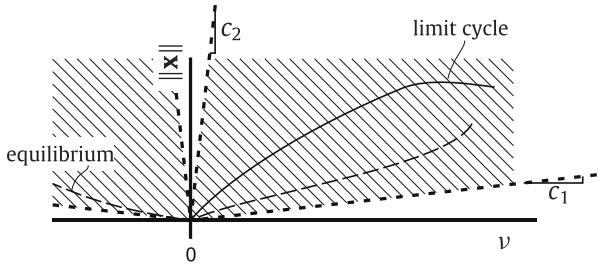

Fig. 2. Exemplary bifurcation diagram with curves for an equilibrium and a limit cycle. Assumption 8 implies that there exist finite $c_1, c_2 > 0$ such that all curves representing limit cycles of (1) are contained in the shaded sectors.

No results are obtained for homoclinic and heteroclinic orbits, or the closed orbits around a center. When such limit sets are not present, then the conewise affine approximation (2) serves as a good local approximation of (1). Theorem 10 shows that equilibria of (1) are accurately represented in the approximation (2). Furthermore, by Theorem 11, limit cycles are accurately represented as well. Therefore, the procedure developed in Section 4 for conewise affine systems is an appropriate tool to study the bifurcations of nonsmooth systems (1). This will be illustrated in Section 6.2 with an example.

6. Illustrative examples

In this section, first we will present a complete bifurcation analysis for a conewise affine system, using the results in the previous sections. Subsequently, we present an example of a nonsmooth system that undergoes two discontinuity-induced bifurcations of an equilibrium point.

6.1. Example for a conewise affine system

Consider the continuous system:

$$\dot{\mathbf{x}} = \begin{cases} A_1\mathbf{x} + \mu\mathbf{b}, & \mathbf{x} \in \mathcal{S}_1 := \{\mathbf{x} \in \mathbb{R}^2 | \mathbf{n}_{41}^T\mathbf{x} < 0 \wedge \mathbf{n}_{12}^T\mathbf{x} > 0\}, \\ A_2\mathbf{x} + \mu\mathbf{b}, & \mathbf{x} \in \mathcal{S}_2 := \{\mathbf{x} \in \mathbb{R}^2 | \mathbf{n}_{12}^T\mathbf{x} < 0 \wedge \mathbf{n}_{23}^T\mathbf{x} > 0\}, \\ A_3\mathbf{x} + \mu\mathbf{b}, & \mathbf{x} \in \mathcal{S}_3 := \{\mathbf{x} \in \mathbb{R}^2 | \mathbf{n}_{23}^T\mathbf{x} < 0 \wedge \mathbf{n}_{34}^T\mathbf{x} > 0\}, \\ A_4\mathbf{x} + \mu\mathbf{b}, & \mathbf{x} \in \mathcal{S}_4 := \{\mathbf{x} \in \mathbb{R}^2 | \mathbf{n}_{34}^T\mathbf{x} < 0 \wedge \mathbf{n}_{41}^T\mathbf{x} > 0\}, \end{cases} \tag{11}$$

where the normal vectors are chosen as $\mathbf{n}_{12} = \begin{bmatrix} 0 & 1 \end{bmatrix}^T$, $\mathbf{n}_{23} = \frac{1}{\sqrt{2}}\begin{bmatrix} -1 & -1 \end{bmatrix}^T$, $\mathbf{n}_{41} = \begin{bmatrix} 0 & -1 \end{bmatrix}^T$, $\mathbf{n}_{23} = \frac{1}{\sqrt{2}}\begin{bmatrix} 1 & 1 \end{bmatrix}^T$. The vector $\mathbf{b} = \begin{bmatrix} \cos(0.375\pi) & \sin(0.375\pi) \end{bmatrix}^T$ and $\mu \in \mathbb{R}$ is the bifurcation parameter. The phase portrait of this system with $\mu = -0.5$ is shown in Fig. 3. The matrices A_i are $A_1 = \begin{bmatrix} -0.5 & 1 \\ -1 & 0 \end{bmatrix}$, $A_2 = \begin{bmatrix} -0.5 & 0.91 \\ -1 & 0.58 \end{bmatrix}$, $A_3 = \begin{bmatrix} -1 & 0.41 \\ 0.5 & 2.08 \end{bmatrix}$, $A_4 = \begin{bmatrix} -1 & 0.5 \\ 0.5 & 1.5 \end{bmatrix}$. System (11) will be analysed with the procedure given in Section 4.3:

1. For $\mu < 0$, two equilibria exist, with positions $\mathbf{x} = -\mu A_2^{-1}\mathbf{b}$ in $\mathcal{S}_2$ and $\mathbf{x} = -\mu A_4^{-1}\mathbf{b}$ in $\mathcal{S}_4$. For $\mu > 0$, no equilibria exist.
2. At $\mu = 0$, the conewise linear dynamics is unstable, since the visible eigenvector in $\mathcal{S}_4$ corresponds to an unstable eigenvalue. In addition, one visible eigenvector in $\mathcal{S}_3$ exists, that corresponds to a stable eigenvalue.
3. Now, the system will be analysed for an arbitrarily chosen negative, and an arbitrarily chosen positive parameter μ. Subsequently, with application of Lemma 7 the complete bifurcation diagram is obtained. For $\mu = -0.5$:
   (a) On Σ_{12}, Σ_{34} and Σ_{41}, there exist points where the vector field is tangent to the boundary, i.e. points $\mathcal{T}_{12}$, $\mathcal{T}_{34}$ and $\mathcal{T}_{41}$, respectively. Trajectories through these points and the origin are shown in Fig. 3. An unstable focus exist in $\mathcal{S}_2$, since the related eigenvalues of A_2 are $0.42 \pm 0.79\imath$, where $\imath^2 = -1$. A saddle point exist in $\mathcal{S}_4$ with eigenvalues -1.10 and 1.60. The stable and unstable manifolds of this point are shown and do not form a homoclinic orbit.
   (b) The trace $\mathrm{tr}(A_1) < 0$, whereas all other traces satisfy $\mathrm{tr}(A_i) > 0$, $i = 2, 3, 4$. Therefore, application of Theorem 2 yields that each possible closed orbit visits $\mathcal{S}_1$. To satisfy Theorem 1, closed orbit(s) should encircle the focus without encircling the saddle point.
   By studying the depicted trajectories, one can conclude, that no closed orbit can traverse $\Sigma_{12} \setminus [O, a]$, since these trajectories cannot encircle the focus without encircling the saddle point, which is required according to Theorem 1. Furthermore, closed orbits cannot traverse the interior of the line $[a, b]$, since trajectories through this open line will arrive at the line $[c, d]$ in finite time, and enter the positively invariant region that is depicted gray in Fig. 3. Now, one can conclude, that possible closed orbits visit only the regions $\mathcal{S}_1$ and $\mathcal{S}_2$, such that they should be contained in the domain, that is depicted gray. This implies, that all closed orbits traverse the line $[\mathcal{T}_{12}, e]$.

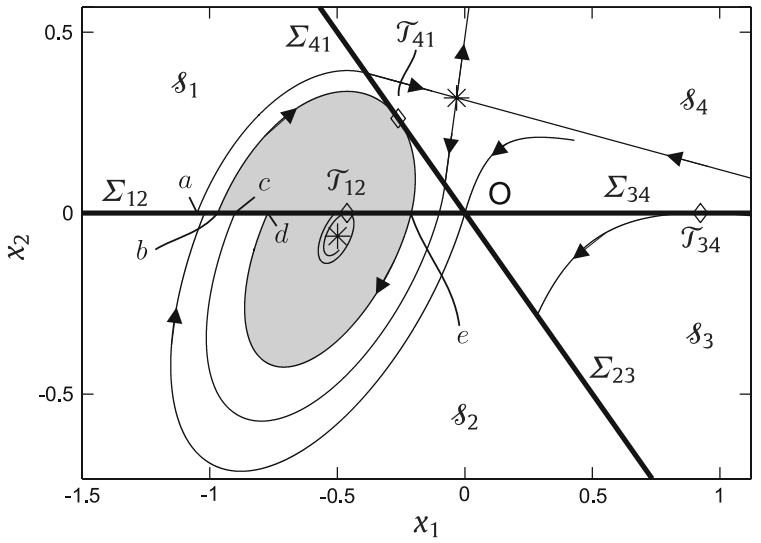

Fig. 3. Phase portrait of system (11) for $\mu = -0.5$ with trajectories through the points $\mathcal{T}_{ij}$, denoted with diamonds, and the origin. In addition, the equilibria are depicted with asterisks, and the manifolds of the saddle point are shown.

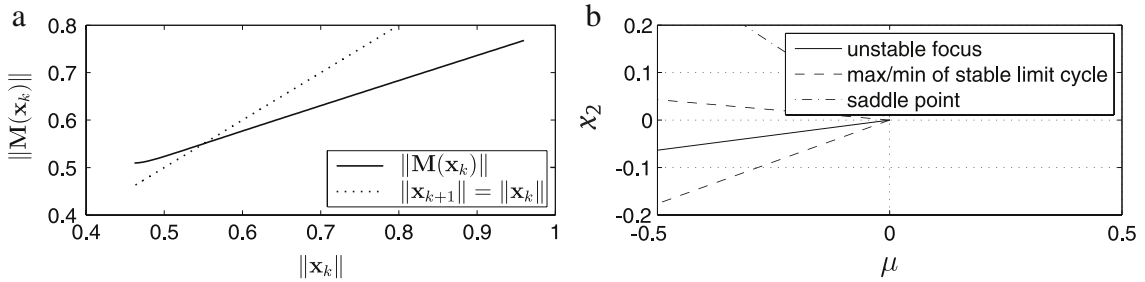

Fig. 4. (a) Combined map M of (11) with $\mu = -0.5$. (b) Bifurcation diagram of (11) with the bifurcation parameter μ.

(c) Existing closed orbits should traverse the line $[\mathcal{T}_{12}, e]$. We construct a map $\mathbf{g}_2 : [\mathcal{T}_{12}, e] \to [d, \mathcal{T}_{12}]$, that yields the position $\mathbf{g}_2(\mathbf{x})$ where a trajectory leaves the cone $\mathcal{S}_2$ when this cone was entered at $\mathbf{x}$. Similarly, the map $\mathbf{g}_1 : [b, \mathcal{T}_{12}] \to [\mathcal{T}_{12}, e]$ is computed. The maps are computed as presented in Appendix A. The combined map $M := \mathbf{g}_1 \circ \mathbf{g}_2(\mathbf{x})$ is the return map and is shown in Fig. 4(a). It contains one fixed point. Apparently, a unique stable limit cycle exists that contains $\mathbf{x} = \begin{pmatrix}-0.55 & 0\end{pmatrix}^T$.

For $\mu = 0.5$ no equilibrium point of (11) exists, such that according to Theorem 1, no closed orbits can exist.

4. With the analysis above and application of Lemma 7, the bifurcation diagram is constructed, as given in Fig. 4(b). Both the limit cycle, focus and saddle exist only for $\mu < 0$. For $\mu = 0$, unstable behaviour is observed. We note that this bifurcation cannot occur in smooth dynamical systems and is explicitly induced by the nonsmoothness of the system.

6.2. Example for a piecewise smooth system

In the following example, a piecewise smooth system is studied that undergoes two bifurcations of an equilibrium. Using the procedure presented in this paper, a local analysis of these bifurcations is performed. For the conewise affine approximations, this analysis guarantees to find all equilibria and limit cycles that are created or destroyed locally during the bifurcations. According to Theorems 10 and 11, the local bifurcations of the piecewise smooth system are accurately described.

We consider the following continuous piecewise smooth system:

$$\dot{\mathbf{x}} = \mathbf{F}_i(\mathbf{x}, \nu), \quad \mathbf{x} \in \mathcal{D}_i, \ i = 1, 2, 3, \tag{12}$$

where $\mathbf{x} = \begin{bmatrix}x_1 & x_2\end{bmatrix}^T \in \mathbb{R}^2$, $\nu \in \mathbb{R}$ is the bifurcation parameter and

$$\mathbf{F}_1(\mathbf{x}, \nu) = \mathcal{A}_1\mathbf{x} + \nu\mathbf{b} + 0.1\begin{bmatrix}0\\ x_1^3\end{bmatrix}, \tag{13}$$

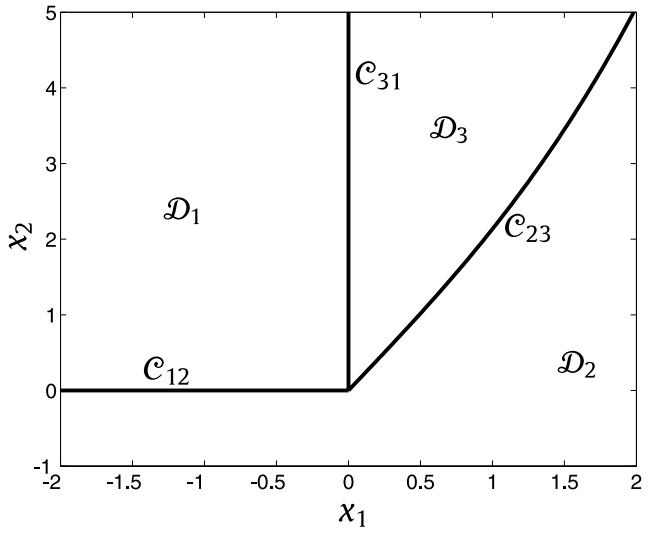

Fig. 5. State space of (12) with boundaries $\mathcal{C}_{ij}$ and domains $\mathcal{D}_i,\ i = 1, 2, 3$.

$$\mathbf{F}_2(\mathbf{x}, \nu) = \mathcal{A}_2\mathbf{x} + \nu\mathbf{b} + 0.1\begin{bmatrix}0\\ x_1^3\end{bmatrix}, \tag{14}$$

$$\mathbf{F}_3(\mathbf{x}, \nu) = \mathcal{A}_3\mathbf{x} + \nu\mathbf{b}, \tag{15}$$

and $\mathcal{A}_1 = \begin{bmatrix}0.5 & -1\\ 1 & 0\end{bmatrix}$, $\mathcal{A}_2 = \begin{bmatrix}0.5 & -1\\ 1 & -0.75\end{bmatrix}$, $\mathcal{A}_3 = \begin{bmatrix}0.5 & -1\\ -0.5 & 0\end{bmatrix}$. The vector $\mathbf{b} = \begin{bmatrix}\cos(0.375\pi) & \sin(0.375\pi)\end{bmatrix}^T$. The domains $\mathcal{D}_i,\ i = 1, 2, 3$, are given by

$$\mathcal{D}_1 = \{\mathbf{x} \in \mathbb{R}^2 | \mathbf{n}_{31}^T\mathbf{x} < 0 \wedge \mathbf{n}_{12}^T\mathbf{x} > 0\}, \tag{16}$$

$$\mathcal{D}_2 = \{\mathbf{x} \in \mathbb{R}^2 | \mathbf{n}_{12}^T\mathbf{x} < 0 \vee h_{23}(\mathbf{x}) < 0\}, \tag{17}$$

$$\mathcal{D}_3 = \{\mathbf{x} \in \mathbb{R}^2 | \mathbf{n}_{31}^T\mathbf{x} > 0 \wedge h_{23}(\mathbf{x}) > 0\}, \tag{18}$$

where the function $h_{23}(\mathbf{x})$ is defined to describe the boundary between $\mathcal{D}_2$ and $\mathcal{D}_3$:

$$h_{23}(\mathbf{x}) := x_2 - \frac{4}{30}x_1^3 - 2x_1, \tag{19}$$

$\mathbf{n}_{31} = \begin{bmatrix}1 & 0\end{bmatrix}^T$ and $\mathbf{n}_{12} = \begin{bmatrix}0 & 1\end{bmatrix}^T$. The boundary between $\mathcal{D}_i$ and $\mathcal{D}_j$ is called $\mathcal{C}_{ij}$. The partitioning of the state space of this piecewise smooth system is depicted in Fig. 5.

First, we study at what parameters an equilibrium point is coinciding with one or more boundaries. An equilibrium point is positioned at the origin at $\nu = 0$. The origin is coinciding with all boundaries. Furthermore, at $\nu = \nu_1$, where $\nu_1 \approx 1.88$, the equilibrium point is positioned on $\mathbf{x} = \mathbf{x}^* \in \mathcal{C}_{12}$, where $\mathbf{x}^* \approx \begin{pmatrix}-1.44 & 0\end{pmatrix}^T$.

For $\nu < \nu_1,\ \nu \neq 0$, an isolated equilibrium exists in $\mathcal{D}_2$. For $\nu > \nu_1$, an equilibrium point exists in $\mathcal{D}_1$. No equilibrium point can exist in $\mathcal{D}_3$.

The equilibria in these domains will not undergo smooth bifurcations, since the Jacobian $J_1(\mathbf{x}, \nu) = \frac{\partial \mathbf{F}_1(\mathbf{x},\nu)}{\partial \mathbf{x}}$ has eigenvalues $\frac{1}{4} \pm \imath\frac{1}{2}\sqrt{3.75 + 1.2x_1^2}$, such that if an equilibrium exists in $\mathcal{D}_1$, then it always is an unstable focus. Furthermore, the Jacobian $J_2(\mathbf{x}, \nu) = \frac{\partial \mathbf{F}_2(\mathbf{x},\nu)}{\partial \mathbf{x}}$ of $\mathbf{F}_2$ has eigenvalues $-\frac{1}{8} \pm \imath\frac{1}{2}\sqrt{2.4375 + 1.2x_1^2}$, such that if an equilibrium exists in $\mathcal{D}_2$, then it always is a stable focus.

The nonsmooth bifurcations around $\nu = 0$ and $\nu = \nu_1$ will be studied locally with a conewise affine approximation of the vector field.

6.2.1. Local analysis around $\nu = 0$

For $\nu = 0$ an equilibrium of (12) exists at the origin and the partial derivative $\frac{\partial \mathbf{F}}{\partial \nu} = \mathbf{b}$, such that Assumptions 1 and 2 are satisfied. Therefore, we approximate the boundaries $\mathcal{C}_{12}$, $\mathcal{C}_{23}$, $\mathcal{C}_{31}$ with the halflines Σ_{12}, Σ_{23} and Σ_{31}, respectively. Here, the vectors $\mathbf{t}_{12} = \begin{pmatrix}-1 & 0\end{pmatrix}^T$, $\mathbf{t}_{23} = \frac{1}{\sqrt{5}}\begin{pmatrix}1 & 2\end{pmatrix}^T$ and $\mathbf{t}_{31} = \begin{pmatrix}0 & 1\end{pmatrix}^T$ define the halflines $\Sigma_{ij} := \{\mathbf{x} \in \mathbb{R}^2 | \mathbf{x} = c\mathbf{t}_{ij}, c \in [0, \infty)\}$. Definition of the normal vectors $\mathbf{n}_{ij} := (\mathbf{e}_1\mathbf{e}_2^T - \mathbf{e}_2\mathbf{e}_1^T)\mathbf{t}_{ij}$ yields $\mathbf{n}_{12} = \begin{pmatrix}0 & 1\end{pmatrix}^T$, $\mathbf{n}_{23} = \frac{1}{\sqrt{5}}\begin{pmatrix}2 & -1\end{pmatrix}^T$ and $\mathbf{n}_{31} = \begin{pmatrix}1 & 0\end{pmatrix}^T$. The state space of this system is given in Fig. 6.

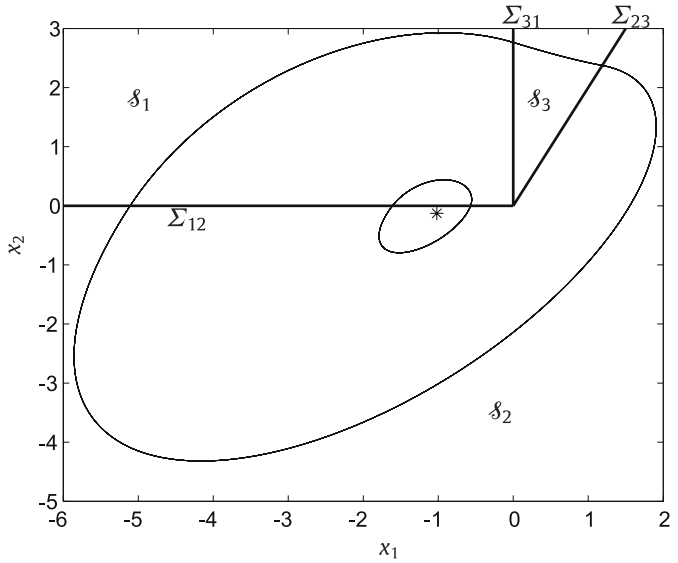

Fig. 6. Limit cycles of (20), where $\mu = 1$. The inner limit cycle is unstable, the outer limit cycle is stable. The stable focus is depicted with an asterisk. According to Theorems 10 and 11, this phase portrait is locally a good approximation for the system (12) for ν in a neighbourhood of 0.

Introducing Taylor expansions of the vector fields $\mathbf{F}_i$, $i = 1, 2, 3$, near the origin, Eq. (12) is locally approximated with:

$$\dot{\mathbf{x}} = \begin{cases} A_1\mathbf{x} + \mu\mathbf{b}, & \mathbf{x} \in \mathcal{S}_1 = \{\mathbf{x} \in \mathbb{R}^2 | \mathbf{n}_{13}^T\mathbf{x} < 0 \wedge \mathbf{n}_{12}^T\mathbf{x} > 0\}, \\ A_2\mathbf{x} + \mu\mathbf{b}, & \mathbf{x} \in \mathcal{S}_2 = \{\mathbf{x} \in \mathbb{R}^2 | \mathbf{n}_{12}^T\mathbf{x} < 0 \vee \mathbf{n}_{23}^T\mathbf{x} > 0\}, \\ A_3\mathbf{x} + \mu\mathbf{b}, & \mathbf{x} \in \mathcal{S}_3 = \{\mathbf{x} \in \mathbb{R}^2 | \mathbf{n}_{23}^T\mathbf{x} < 0 \wedge \mathbf{n}_{13}^T\mathbf{x} > 0\}, \end{cases} \tag{20}$$

where $A_i = \mathcal{A}_i$, $i = 1, 2, 3$, the affine vector is given by $\mathbf{b} = \begin{bmatrix}\cos(0.375\pi) & \sin(0.375\pi)\end{bmatrix}^T$ and $\mu = \nu$ is the bifurcation parameter.

The conewise affine system (20) is analysed with the procedure presented in Section 4.3. This analysis is completely analogous to the analysis of the example given in Section 6.1. For the sake of brevity we omit the detailed analysis here and focus on the discussion of the results; see [19] for further details.

At $\mu = 0$, a stable spiralling motion is observed, such that the origin is a stable equilibrium point. For all $\mu \neq 0$, only one equilibrium exists, that is positioned in $\mathcal{S}_2$ and is a stable focus. For negative parameters μ, using a halfline R as defined in Theorem 8, we obtain that no periodic orbits exist, such that only a single, stable focus exists. For positive parameters μ, the system (20) contains two limit cycles and a stable focus, that are depicted in Fig. 6 for $\mu = 1$. With the return maps that are derived in this paper, we obtain that the inner limit cycle is unstable, the outer limit cycle is stable.

The bifurcation diagram of (20) is depicted in Fig. 8a for the parameter range $\mu \in [-0.8, 0.8]$, that corresponds to the same range of the system parameter ν of (12).

6.2.2. Local analysis around $\nu = \nu_1$

For $\nu = \nu_1$, an equilibrium point $\mathbf{x}^*$ exists that satisfies $\mathbf{x}^* \in \Sigma_{12}$. We consider the neighbourhood around the bifurcation point, and therefore introduce $\mu = \nu - \nu_1$ and $\mathbf{y} := \mathbf{x} - \mathbf{x}^*$, where $\mathbf{y} = \begin{pmatrix}\mathbf{y}_1 & \mathbf{y}_2\end{pmatrix}^T$. The partial derivative $\frac{\partial \mathbf{F}}{\partial \nu} = \mathbf{b}$, such that Assumptions 1 and 2 are satisfied.

We approximate the boundary $\mathcal{C}_{12}$ with the halflines Σ_{12p}, and Σ_{12n}, where Σ_{12p} and Σ_{12n} describes the boundary $\mathcal{C}_{12}$ for $\mathbf{x}_1 \geq \mathbf{x}_1^*$ and $\mathbf{x}_1 \leq \mathbf{x}_1^*$, respectively. Let the unit vectors $\mathbf{t}_{12p} = \begin{pmatrix}1 & 0\end{pmatrix}^T$ and $\mathbf{t}_{12n} = \begin{pmatrix}-1 & 0\end{pmatrix}^T$ define the halflines $\Sigma_{12p} := \{\mathbf{y} \in \mathbb{R}^2 | \mathbf{y} = c\mathbf{t}_{12p}, c \in [0, \infty)\}$ and $\Sigma_{12n} := \{\mathbf{y} \in \mathbb{R}^2 | \mathbf{y} = c\mathbf{t}_{12n}, c \in [0, \infty)\}$. The normal vectors are $\mathbf{n}_{12p} = \begin{pmatrix}0 & -1\end{pmatrix}^T$ and $\mathbf{n}_{12n} = \begin{pmatrix}0 & 1\end{pmatrix}^T$.

Introducing a Taylor expansion of the vector fields $\mathbf{F}_i$, $i = 1, 2$, near the point $(\mathbf{x}^*, \nu_1)$, system (12) is locally approximated with:

$$\dot{\mathbf{y}} = \begin{cases} A_1\mathbf{y} + \mu\mathbf{b}, & y \in \mathcal{S}_1 = \{\mathbf{y} \in \mathbb{R}^2 | \mathbf{n}_{12p}^T\mathbf{y} < 0\}, \\ A_2\mathbf{y} + \mu\mathbf{b}, & y \in \mathcal{S}_2 = \{\mathbf{y} \in \mathbb{R}^2 | \mathbf{n}_{12p}^T\mathbf{y} > 0\}, \end{cases} \tag{21}$$

where $A_1 = \left(\mathcal{A}_1 + \begin{pmatrix}0 & 0 \\ 0.3(\mathbf{x}_1^*)^2 & 0\end{pmatrix}\right)$ and $A_2 = \left(\mathcal{A}_2 + \begin{pmatrix}0 & 0 \\ 0.3(\mathbf{x}_1^*)^2 & 0\end{pmatrix}\right)$, where the affine vector is given by $\mathbf{b} = \begin{bmatrix}\cos(0.375\pi) & \sin(0.375\pi)\end{bmatrix}^T$ and $\mu \in \mathbb{R}$ is the bifurcation parameter.

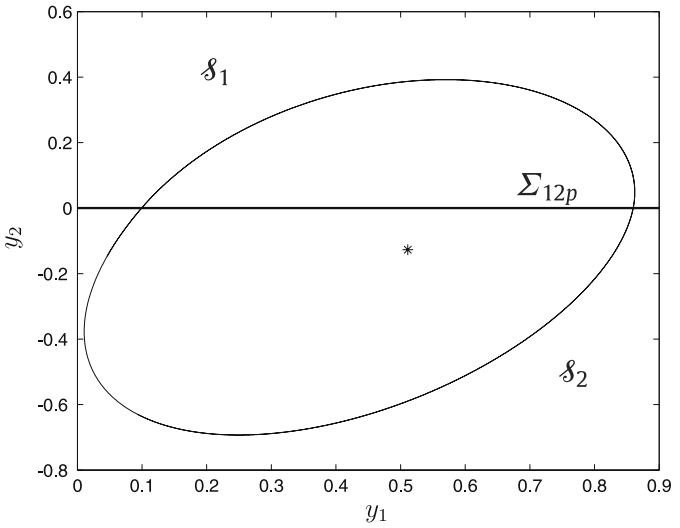

Fig. 7. Unstable limit cycle of (21) with $\mu = -1$. The stable focus is depicted with an asterisk.

Once more, for details of the analysis of bifurcations of (21) using the procedure of Section 4, we refer to [19]. Here we focus on discussing the results. For $\mu < 0$, one equilibrium point exists in $\mathcal{S}_2$, that is a stable focus. This focus is encircled by an unstable limit cycle, as depicted in Fig. 7 for $\mu = -1$. At $\mu = 0$, an expanding spiralling motion is observed around the origin, such that the equilibrium at the origin is unstable. For $\mu > 0$, one equilibrium point exist in $\mathcal{S}_2$, and no limit cycles exist.

The bifurcation diagram is depicted in Fig. 8a for the parameter range $\mu \in [-0.8, 0.8]$, that corresponds to the range of the system parameters $\nu \in [1.08, 2.68]$ of system (12). This type of bifurcation was identified in [7] as a *discontinuous Hopf* bifurcation.

6.2.3. Bifurcations of the nonsmooth system

The nonsmooth bifurcations around $\nu = 0$ and $\nu = \nu_1$ are approximated locally in the previous sections, yielding the bifurcation diagram as depicted in Fig. 8a. According to Theorems 10 and 11, similar limit sets exist in the smooth system (12). Using the approximations, the bifurcation diagram of (12) is given in Fig. 8b and Fig. 8c. The limit cycles created or destroyed by the bifurcations, as found by the conewise affine approximations, are followed for varying $\nu \neq 0$ and $\nu \neq \nu_1$ using a sequential implementation of the shooting algorithm, cf. [20]. The path of the equilibrium point is computed analytically.

The local bifurcations of the equilibrium at $\nu = 0$ and $\nu = \nu_1$ are accurately described. However, since the conewise affine approximation uses a *local* approximation of (12) near $(\nu, \mathbf{x}) = (\nu_1, \mathbf{x}^*)$, the stable limit cycle induced at $\nu = 0$ is not identified by the local approximation around $\nu = \nu_1$.

Note that the approach of this paper does not yield information on bifurcations of limit cycles. For example, with the presented analysis we cannot exclude a bifurcation of the stable limit cycle for $\nu > 0$.

7. Conclusions

A procedure is presented that yields a complete analysis of bifurcating equilibria in a class of hybrid systems, described by a continuous, piecewise smooth differential equations. This procedure is a computationally feasible method to identify all limit sets that are created or destroyed during the bifurcation of an equilibrium point.

To analyse the bifurcation with the given procedure, under certain assumptions, continuous, piecewise smooth hybrid systems can be approximated near the bifurcation point by a conewise affine system. The bifurcation of the approximated, conewise affine system accurately describes the local bifurcation of the equilibrium point in the continuous, piecewise smooth system.

For the conewise affine system we study what limit sets appear or disappear, change in character or in their stability properties under change of a system parameter. Existing equilibria, homoclinic and heteroclinic orbits of the conewise affine system can be found in a relatively straightforward manner. The other limit sets that are possible in autonomous planar systems are closed orbits, including limit cycles. To find these, we study the Poincaré return maps.

To be able to find all limit sets in a computationally feasible manner, new theoretical results are presented. With these results, one can exclude the existence of closed orbits far away from the equilibria. Using these theoretical results, the presented procedure is able to identify, in a computationally efficient manner, all limit sets, which appear or disappear in the discontinuity-induced bifurcation of the equilibrium of the approximated, conewise affine system. The procedure will

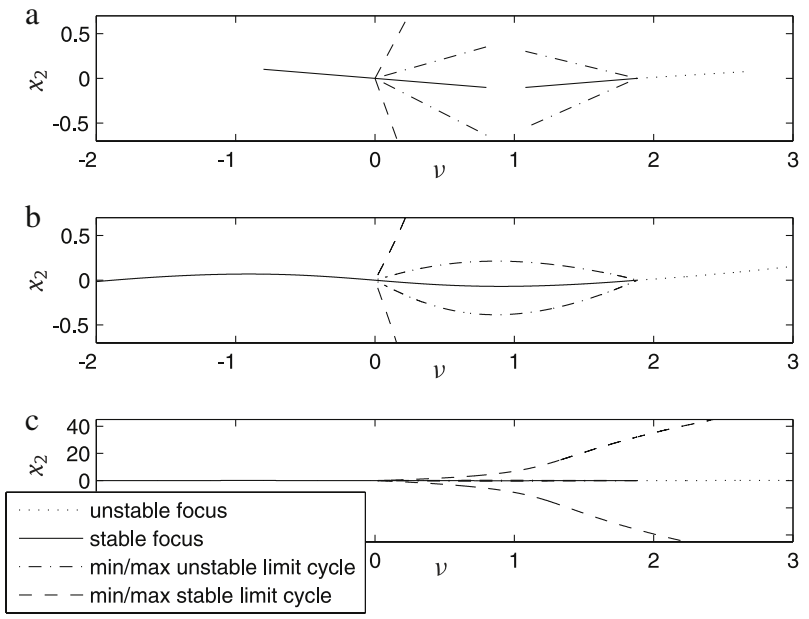

Fig. 8. Application of conewise affine approximations for the bifurcation analysis of (12). In panel a, the limit sets are shown of the conewise affine approximations at $\nu = 0$ and $\nu = \nu_1$. In panel b, the equilibrium path of (12) is shown, which is computed analytically. Furthermore, the limit cycles are computed by repeated application of the shooting method. Since the stable limit cycle grows in 'amplitude' with increasing ν, the contents of panel b is repeated in panel c with a larger y-scale.

identify all closed orbits, when multiple closed orbits are created at the bifurcation point. In two examples, the theoretical results are illustrated.

The procedure presented in this paper is useful to assess the parameter dependency of the dynamics of planar piecewise smooth systems. Knowledge on what limit sets can appear or disappear under parameter changes of a system can be useful in the design of a system that is nonsmooth, and can be used to evaluate the robustness of the system, which is generally an important desired characteristic for nonsmooth control systems.

The results of this work can be extended to a more general class of hybrid systems, described by piecewise smooth systems with a discontinuous right-hand side, which are relevant for example in the context of mechanical systems with Coulomb friction.

Acknowledgements

This work is supported by the European Network of Excellence HYCON (FP6-IST-511368) and by the Netherlands Organisation for Scientific Research (NWO).

Appendix A. Computation of maps $\mathbf{g}_i$, $i = 1, \ldots, m$.

We study a trajectory traversing $\mathcal{S}_i$ from the boundary Σ_- towards the boundary Σ_+ in a finite time t_i. Therefore, the trajectory $\mathbf{x}(t)$ satisfies $\mathbf{x}(t) \in \mathcal{S}_i$, $t \in (0, t_i)$, $\mathbf{x}(0) \in \Sigma_-$ and $\mathbf{x}(t_i) \in \Sigma_+$. To analyse this trajectory in the cone $\mathcal{S}_i$, a new coordinate frame will be used, whose origin is shifted to the point where $A_i\mathbf{x} + \mu\mathbf{b} = \mathbf{0}$. In addition, other basis vectors are chosen to describe positions in $\mathbb{R}^2$. The relations between coordinates in the original frame, denoted as $\mathbf{x}$, with coordinates in the new frame, denoted as $\tilde{\mathbf{x}}^i$, are:

$$\tilde{\mathbf{x}}^i = P_i^{-1}\mathbf{x} + \mu P_i^{-1}A_i^{-1}\mathbf{b}, \qquad \mathbf{x} = P_i\tilde{\mathbf{x}}^i - \mu A_i^{-1}\mathbf{b}, \tag{22}$$

where P_i is found by the real Jordan decomposition, such that $A_i = P_iJ_iP_i^{-1}$. The dynamics expressed in the new coordinate frame is given by:

$$\dot{\tilde{\mathbf{x}}}^i = J_i\tilde{\mathbf{x}}^i, \quad \text{for } t \in [0, t_i]. \tag{23}$$

Consider an initial condition with coordinates $\mathbf{x}_0 = p^i\mathbf{t}_- \in \Sigma_-$. In the new coordinate frame, one finds $\tilde{\mathbf{x}}_0^i = P_i^{-1}(p^i\mathbf{t}_- + \mu A_i^{-1}\mathbf{b})$. The direction of the vector tangent to the boundary Σ_- is given by $\tilde{\mathbf{t}}_-^i := P_i^{-1}\mathbf{t}_-$, such that $\tilde{\mathbf{x}}_0^i = p^i\tilde{\mathbf{t}}_-^i + \mu P_i^{-1}A_i^{-1}\mathbf{b}$.

There exists a crossing of the trajectory with the boundary Σ_+ at time t_i. Suppose this crossing occurs at $\mathbf{x}(t_i) = p^{i+1}\mathbf{t}_+$. In the new coordinate frame, this position is given by $\tilde{\mathbf{x}}^i(t_i) = p^{i+1}\tilde{\mathbf{t}}^i_+ + \mu P_i^{-1}A_i^{-1}\mathbf{b}$, where a vector $\tilde{\mathbf{t}}^i_+ := P_i^{-1}\mathbf{t}_+$ is introduced, that is parallel with Σ_+. Defining a vector orthogonal to $\tilde{\mathbf{t}}^i_+$ yields $\tilde{\mathbf{n}}^i_+ := (\mathbf{e}_1\mathbf{e}_2^T - \mathbf{e}_2\mathbf{e}_1^T)\tilde{\mathbf{t}}^i_+$, such that:

$$\tilde{\mathbf{n}}^{iT}_+\tilde{\mathbf{x}}^i(t_i) = \mu\tilde{\mathbf{n}}^{iT}_+P_i^{-1}A_i^{-1}\mathbf{b}. \tag{24}$$

Substitution of the solution $\tilde{\mathbf{x}}^i(t) = \mathrm{e}^{J_it}\tilde{\mathbf{x}}^i_0$ of (23) in (24) yields an expression which is evaluated at the time t_i:

$$\tilde{\mathbf{n}}^{iT}_+\mathrm{e}^{J_it_i}\tilde{\mathbf{x}}^i_0 = \tilde{\mathbf{n}}^{iT}_+\tilde{\mathbf{x}}^i_T, \tag{25}$$

where we defined the translation vector $\tilde{\mathbf{x}}^i_T := \mu P_i^{-1}A_i^{-1}\mathbf{b}$.

When the traversal time t_i satisfying (25) is found, this time can be used to obtain the traversal position. Integrating (23) over a time interval $[0, t_i]$ yields $\tilde{\mathbf{x}}^i(t_i) = \mathrm{e}^{J_it_i}\tilde{\mathbf{x}}^i_0$. In the original coordinate frame, this yields:

$$\mathbf{x}(t_i) = P_i\mathrm{e}^{J_it_i}\tilde{\mathbf{x}}^i_0 - \mu A_i^{-1}\mathbf{b}. \tag{26}$$

Substitution of the time t_i satisfying (25) in (26) forms a map $\mathbf{g_i} : D_i \subset \Sigma_- \to R_i \subset \Sigma_+$, describing the position of the crossing position of the trajectory $\{\mathbf{x}(t),\ t > 0,\ \mathbf{x}(0) \in D_i\}$ with Σ_+, such that $\mathbf{x}(t_i) = \mathbf{g}_i(\mathbf{x}(0))$. The map $\mathbf{g}_i$ will be computed by distinguishing the three cases.

Case 1: If A_i has complex eigenvalues, then $J_i = \begin{bmatrix} a_i & -\omega_i \\ \omega_i & a_i \end{bmatrix}$, where a_i and ω_i are real and $\omega_i > 0$. Hence, $\mathrm{e}^{J_it} = \mathrm{e}^{a_it}\begin{bmatrix} \cos(\omega_it) & -\sin(\omega_it) \\ \sin(\omega_it) & \cos(\omega_it) \end{bmatrix}$. Herewith, (25) yields:

$$\mathrm{e}^{a_it_i}\cos(\omega_it_i)\tilde{\mathbf{n}}^{iT}_+\tilde{\mathbf{x}}^i_0 + \mathrm{e}^{a_it_i}\sin(\omega_it_i)\tilde{\mathbf{t}}^{iT}_+\tilde{\mathbf{x}}^i_0 = \tilde{\mathbf{n}}^{iT}_+\tilde{\mathbf{x}}^i_T. \tag{27}$$

This equation can be solved with a numerical solver to obtain the time t_i. This time yields the position:

$$\mathbf{x}(t_i) = -\mathrm{e}^{a_it_i}\sin(\omega_it_i)P_i\left(\mathbf{e}_1\mathbf{e}_2^T - \mathbf{e}_2\mathbf{e}_1^T\right)\tilde{\mathbf{x}}^i_0 + \mathrm{e}^{a_it_i}\cos(\omega_it_i)P_i\tilde{\mathbf{x}}^i_0 - \mu A_i^{-1}\mathbf{b}. \tag{28}$$

Case 2: If A_i has two real eigenvalues λ_{ai} and λ_{bi} whose eigenvectors are distinct, then $J_i = \begin{bmatrix} \lambda_{ai} & 0 \\ 0 & \lambda_{bi} \end{bmatrix}$. Using $\mathrm{e}^{J_it} = \mathrm{e}^{\lambda_{ai}t}\mathbf{e}_1\mathbf{e}_1^T + \mathrm{e}^{\lambda_{bi}t}\mathbf{e}_2\mathbf{e}_2$, we obtain: $\tilde{\mathbf{x}}^i(t) = \mathrm{e}^{\lambda_{ai}t}\mathbf{e}_1\mathbf{e}_1^T\tilde{\mathbf{x}}^i_0 + \mathrm{e}^{\lambda_{bi}t}\mathbf{e}_2\mathbf{e}_2^T\tilde{\mathbf{x}}^i_0$, such that (25) becomes:

$$\mathrm{e}^{\lambda_{ai}t_i}\tilde{\mathbf{n}}^{iT}_+\mathbf{e}_1\mathbf{e}_1^T\tilde{\mathbf{x}}^i_0 + \mathrm{e}^{\lambda_{bi}t_i}\tilde{\mathbf{n}}^{iT}_+\mathbf{e}_2\mathbf{e}_2^T\tilde{\mathbf{x}}^i_0 = \tilde{\mathbf{n}}^{iT}_+\tilde{\mathbf{x}}^i_T, \tag{29}$$

that can be solved with a numerical solver to obtain the smallest time $t_i > 0$. Evaluating (26) on this time yields:

$$\mathbf{x}(t_i) = \mathrm{e}^{\lambda_{ai}t}P_i\mathbf{e}_1\mathbf{e}_1^T\tilde{\mathbf{x}}^i_0 + \mathrm{e}^{\lambda_{bi}t}P_i\mathbf{e}_2\mathbf{e}_2^T\tilde{\mathbf{x}}^i_0 - \mu A_i^{-1}\mathbf{b}. \tag{30}$$

Case 3: If A_i has two equal real eigenvalues λ_{ai} with geometric multiplicity 1, then $J_i = \begin{bmatrix} \lambda_{ai} & 1 \\ 0 & \lambda_{ai} \end{bmatrix}$ and $\mathrm{e}^{J_it} = \mathrm{e}^{\lambda_{ai}t}\begin{bmatrix} 1 & t \\ 0 & 1 \end{bmatrix}$. Substituting this expression in (25) yields:

$$\mathrm{e}^{\lambda_{ai}t_i}\tilde{\mathbf{n}}^{iT}_+\tilde{\mathbf{x}}^i_0 + t_i\mathrm{e}^{\lambda_{ai}t_i}\tilde{\mathbf{n}}^{iT}_+\mathbf{e}_1\mathbf{e}_2^T\tilde{\mathbf{x}}^i_0 = \tilde{\mathbf{n}}^{iT}_+\tilde{\mathbf{x}}^i_T. \tag{31}$$

When the smallest $t_i > 0$ satisfying (31) is found with a numerical solver, this can be substituted in (26), yielding:

$$\mathbf{x}(t_i) = \mathrm{e}^{\lambda_{ai}t_i}P_i\tilde{\mathbf{x}}^i_0 + t_i\mathrm{e}^{\lambda_{ai}t_i}P_i\mathbf{e}_1\mathbf{e}_2^T\tilde{\mathbf{x}}^i_0 - \mu A_i^{-1}\mathbf{b}. \tag{32}$$

Appendix B. Proofs

Proof of Theorem 1. First we prove the existence of at least one equilibrium point. For this purpose, the index of a point and the index of a Jordan curve are introduced. Next, we will prove the second part of the theorem.

Let $\Delta\theta$ be the total change in the angle θ that the vector $\mathbf{f}(\mathbf{x})$ makes with some fixed direction as $\mathbf{x}$ traverses a Jordan curve J once in the positive direction. Recall from [10] that a Jordan curve is defined as a topological image of a circle, i.e. J is an $\mathbf{x}$-set of points $\mathbf{x} = \mathbf{x}(t)$, $a \le t \le b$, where $\mathbf{x}(t)$ is continuous, $\mathbf{x}(a) = \mathbf{x}(b)$ and $\mathbf{x}(s) \ne \mathbf{x}(t)$, for $a \le s < t < b$. Define the index of J with respect to $\mathbf{f}$ as $I_{\mathbf{f}}(J) := \frac{\Delta\theta}{2\pi}$.

Define the index of an isolated equilibrium point P with respect to $\mathbf{f}$ as the index of any Jordan curve encircling P, and no other equilibrium points. This index will be denoted by $I_{\mathbf{f}}(P)$. For certain equilibria, the index is known; $I_{\mathbf{f}}(P) = 1$ if P is a hyperbolic node or focus and $I_{\mathbf{f}}(P) = -1$ if P is a hyperbolic saddle.

According to Theorem 4.4, p. 400, [14], since C is a periodic orbit, $I_{\mathbf{f}}(C) = 1$. The periodic orbit C is a Jordan curve, such that Theorem 4.1, p. 398, [14] yields that C encircles at least one equilibrium point. This proves the first statement of the theorem.

Suppose that all equilibrium points $P_1, \ldots P_m$ that are encircled by the closed orbit are hyperbolic. Application of Corollary 2, p. 400, [14] yields that the sum of indices of these equilibria equals one, i.e. $I_{\mathbf{f}}(C) = \sum_{i=1}^{m} I_{\mathbf{f}}(P_i) = 1$. The value of the indices of a node, focus and saddle imply, that there must be an odd number $2n+1$ of equilibria, of which n are saddles and $n+1$ are nodes or foci. □

Proof of Lemma 3. Three cases have to be distinguished according to the eigenvalues of the matrix A, that describes the dynamics $\dot{\mathbf{y}} = A\mathbf{y}$ in region $\bar{\mathcal{S}}$. The existence of a visible eigenvector, corresponding to a real eigenvalue, implies that all eigenvalues of $A \in \mathbb{R}^{2\times 2}$ are real.

In the first case, the eigenvalues of A are equal and this eigenvalue has geometric multiplicity two. The trajectories inside $\bar{\mathcal{S}}$ converge to the origin since $\dot{\mathbf{y}} = A\mathbf{y}$ yields $\mathbf{y}(t) = \mathrm{e}^{\lambda t}\mathbf{y}_0,\ \forall \mathbf{y}_0 \in \bar{\mathcal{S}}$, where $\lambda < 0$.

In the second case, the matrix A has an eigenvalue $\lambda < 0$ with algebraic multiplicity two and geometric multiplicity one. Trajectories starting in $\bar{\mathcal{S}}$ can be written as $\mathbf{y}(t) = P\mathrm{e}^{Jt}P^{-1}\mathbf{y}_0 = \mathrm{e}^{\lambda t}(\mathbf{y}_0 + tP\mathbf{e}_1\mathbf{e}_2^TP^{-1}\mathbf{y}_0)$ as long as $\mathbf{y}(\tau) \in \bar{\mathcal{S}}\ \forall \tau \in [0, t]$, where the Jordan canonical form $A = PJP^{-1}$ is used, with $J = \lambda(\mathbf{e}_1\mathbf{e}_1^T + \mathbf{e}_2\mathbf{e}_2^T) + \mathbf{e}_1\mathbf{e}_2^T$, $\mathbf{e}_1 := \begin{pmatrix}1 & 0\end{pmatrix}^T$ and $\mathbf{e}_2 := \begin{pmatrix}0 & 1\end{pmatrix}^T$. With $\lambda < 0$, either convergence of the trajectory to the origin is obtained, or the trajectory leaves $\bar{\mathcal{S}}$ in finite time.

In the third case, the matrix A has two distinct eigenvalues $\lambda_a < 0$ and $\lambda_b < 0$. Trajectories in the region $\bar{\mathcal{S}}$ are positioned on the equilibrium $\mathbf{y}(t) = \mathbf{0},\ \forall t > 0$ or can be written as $\mathbf{y}(t) = P\mathrm{e}^{Jt}P^{-1}\mathbf{y}_0 = P\mathbf{e}_1\mathbf{e}_1^TP^{-1}\mathbf{y}_0\mathrm{e}^{\lambda_a t} + P\mathbf{e}_2\mathbf{e}_2^TP^{-1}\mathbf{y}_0\mathrm{e}^{\lambda_b t},\ \forall \mathbf{y}_0 \in \bar{\mathcal{S}}$ as long as $\mathbf{y}(\tau) \in \bar{\mathcal{S}},\ \forall \tau \in [0, t]$, where the Jordan canonical form $A = PJP^{-1}$ is used, with $J = \lambda_a\mathbf{e}_1\mathbf{e}_1^T + \lambda_b\mathbf{e}_2\mathbf{e}_2^T$ and $\mathbf{y}_0 \in \bar{\mathcal{S}}$. The eigenvectors of A are given by the vectors $\mathbf{v}_a = P\mathbf{e}_1$ and $\mathbf{v}_b = P\mathbf{e}_2$. The trajectory $\mathbf{y}(t)$ converges to either $I_{va} = \{\mathbf{y} \in \mathbb{R}^2 | \mathbf{y} = c\mathbf{v}_a,\ c \in (0, \infty)\}$ when $\lambda_a > \lambda_b$ or $I_{vb} = \{\mathbf{y} \in \mathbb{R}^2 | \mathbf{y} = c\mathbf{v}_b,\ c \in (0, \infty)\}$ when $\lambda_a < \lambda_b$. If trajectories converge to the set $I_{vk},\ k = a, b$, corresponding to a visible eigenvector, i.e. $I_{vk} \in \bar{\mathcal{S}},\ k = a, b$, they will approach the origin, since the corresponding eigenvalue $\lambda_k < 0,\ k = a, b$. Otherwise, they will leave the region $\bar{\mathcal{S}}$ in finite time. □

Proof of Lemma 4. When $\bar{\mathcal{S}}$ is a halfline, the vector field $A\mathbf{y}$ is pointing out of $\bar{\mathcal{S}}$, since otherwise, all $\mathbf{y} \in \bar{\mathcal{S}} \setminus \{\mathbf{0}\}$ are eigenvectors, that are visible. Every nonempty closed cone $\bar{\mathcal{S}} \subset \mathbb{R}^2$ that is not a halfline can be written as the union of two nonempty closed convex cones $\bar{\mathcal{S}}_1$ and $\bar{\mathcal{S}}_2$ that do not contain a subspace of $\mathbb{R}^2$, i.e. $\bar{\mathcal{S}} = \bar{\mathcal{S}}_1 \cup \bar{\mathcal{S}}_2$, where these cones intersect only at the halfline $\Sigma_{12} = \bar{\mathcal{S}}_1 \cap \bar{\mathcal{S}}_2$. Due to the assumption in Lemma 4, both regions $\bar{\mathcal{S}}_j,\ j = 1, 2$, and the boundary Σ_{12} do not contain an eigenvector of A.

According to Theorem 3 of [13], for any $\mathbf{y}_0 \in \bar{\mathcal{S}}_j,\ j = 1, 2$, with $\mathbf{y}_0 \neq \mathbf{0}$, there exists a time $t_1 \geq 0$ such that $\mathrm{e}^{At_1}\mathbf{y}_0 \notin \bar{\mathcal{S}}_j$. Trajectories can traverse the boundary Σ_{12} only in one direction. Therefore, trajectories from a point $y_0 \in \bar{\mathcal{S}}_j$ leave $\bar{\mathcal{S}}$ in a finite time, possibly after traversing the other cone $\bar{\mathcal{S}}_k, k \in \{1, 2\}, k \neq j$. □

Proof of Lemma 5. Necessity is trivial. To prove sufficiency of the stability requirements, we will prove that for every trajectory $\mathbf{y}(t)$, with initial condition $\mathbf{y}_0 \in \mathbb{R}^2 \setminus \mathbf{0}$, there exist a finite time t_f and closed cone $\bar{\mathcal{S}}_k$, such that $\mathbf{y}(t) \in \bar{\mathcal{S}}_k, \forall t > t_f$. Subsequently, we will prove that the trajectories converge to the origin for $t \to \infty$.

Consider the trajectory from any initial condition $\mathbf{y}_0 \in \mathbb{R}^2 \setminus \mathbf{0}$. When $\mathbf{y}_0$ is inside a cone $\bar{\mathcal{S}}$ containing no visible eigenvectors, Lemma 4 guarantees that the trajectory will leave this cone in a finite time. When $\mathbf{y}_0$ is inside a cone $\bar{\mathcal{S}}$ containing visible eigenvectors, then, according to Lemma 3, trajectories may converge to the origin asymptotically and remain in this cone. In that case, choose $t_1 = 0$. Otherwise, they will leave the cone $\bar{\mathcal{S}}$ in a finite time t_1.

Trajectories can traverse a boundary $\Sigma_{i,i+1} = \{\mathbf{y} \in \mathbb{R}^2 | \mathbf{y} = c\mathbf{t}_{i,i+1},\ c \in (0, \infty)\}$ only in one direction, either from $\mathcal{S}_i$ to $\mathcal{S}_{i+1}$ or vise versa, since the vector field $\mathbf{f}(\mathbf{y})$ on $\mathbf{y} = c\mathbf{t}_{i,i+1}$ is given by $\dot{\mathbf{y}} = cA_i\mathbf{t}_{i,i+1}$ and $c > 0$. This means that possibly after escape or traversal of some regions, all trajectories will arrive at a cone $\bar{\mathcal{S}}_k$ containing a visible eigenvector and remain there for all $t > t_f$. Here, t_f is the sum of the finite time the escape of the first region took, and the finite times for the traversal of regions without visible eigenvectors. Since these times are all finite according to Lemmas 3 and 4, the sum of these, which is defined as t_f, is also finite.

By Lipschitz continuity, the trajectory $\mathbf{y}(t)$ remains bounded for $t \in [0, t_f]$. Subsequently, it remains in a specific cone $\bar{\mathcal{S}}_k$ for all $t > t_f$, where $\bar{\mathcal{S}}_k$ contains a visible eigenvector. Hence, Lemma 3 guarantees asymptotic stability of the origin. □

Proof of Theorem 6. When visible eigenvectors are present, then necessity and sufficiency of (i) is given in Lemma 5. In absence of visible eigenvectors, necessity of (ii) is proven by contradiction. Let T be the period time of the spiralling motion of (3), as given in [13]. When $\Lambda \geq 1$, then a trajectory from $\mathbf{y}_0 \in \Sigma_{m1}$ visits the sequence of positions $\mathbf{y}(kT) = \Lambda^k\mathbf{y}_0,\ k = 1, 2, \ldots$, contradicting asymptotic stability.

Sufficiency of (ii) can be obtained by proving that all trajectories will cross the boundary Σ_{m1} in finite time. After this finite time, the contraction property of the return map $\mathbf{y}_{k+1} = \Lambda\mathbf{y}_k$, with $\Lambda < 1$ implies asymptotic stability.

For trajectories starting with initial conditions positioned in one of the regions $\mathcal{S}_i,\ i = 1, \ldots, m$, according to Lemma 4, there exists a finite time $t_1 \in [0, \infty)$, such that the trajectory is not in the region $\mathcal{S}_i$. Since no state jumps can exist in (3), the trajectory will therefore cross a boundary $\Sigma_{i,i+1}$ in a finite time $t_s \in [0, t_1]$. Each boundary can only be traversed in one direction. Therefore, only a finite number of regions $\mathcal{S}_i$ can be traversed, before Σ_{m1} is reached in a finite time. In this finite time, the trajectory does not grow unbounded since (3) is globally Lipschitz.

After the trajectory has reached Σ_{m1} for the first time, the trajectory converges to the origin in a spiralling motion, as described by the return map $\mathbf{y}_{k+1} = \Lambda\mathbf{y}_k$, due to the fact that $\Lambda < 1$. Herewith, sufficiency of (ii) is proven. □

Proof of Lemma 7. The proof is trivial and omitted for the sake of brevity. □

Proof of Theorem 8. To prove the theorem, first, a scaling law for conewise linear systems is presented in Lemma 12. Second, a relationship between trajectories of the conewise affine system with $\mu \neq 0$ and conewise linear systems with $\mu = 0$ is given in Lemma 13. Using that result, Theorem 8 is proven.

Lemma 12. *Consider two trajectories of the continuous, conewise linear system:*

$$\dot{\mathbf{y}} = \mathbf{f}(\mathbf{y}), \tag{33}$$
$$\mathbf{f}(\mathbf{y}) := A_i\mathbf{y}, \quad \mathbf{y} \in \mathcal{S}_i,\ i = 1, \ldots, m,$$

where $\mathcal{S}_i,\ i = 1, \ldots, m$, are cones. Consider the trajectories for two initial conditions, $\mathbf{y}_0$ and $\tilde{\mathbf{y}}_0$, where $\tilde{\mathbf{y}}_0 = c\mathbf{y}_0,\ c \in [0, \infty)$. If $\mathbf{y}(t)$ is a trajectory for the system with $\mathbf{y}(0) = \mathbf{y}_0$, then $\tilde{\mathbf{y}}(t) = c\mathbf{y}(t)$ is a trajectory emanating from $\tilde{\mathbf{y}}(0) = \tilde{\mathbf{y}}_0$.

Lemma 13. *Consider the continuous, conewise affine system given in (2), with constant $\mu \neq 0$. Suppose this system does not contain visible eigenvectors.*

Define a Poincaré section for this system at the moments where the trajectory $\mathbf{x}(t)$ traverses Σ_{m1} with a specified direction (i.e. either from $\mathcal{S}_m$ to $\mathcal{S}_1$ or vise versa). Define the return map $M : D_M \subset \Sigma_{m1} \to I_M \subset \Sigma_{m1}$, such that $M(\mathbf{x}_k)$ denotes the position of the first crossing of $\mathbf{x}(t),\ t > 0$, for the initial condition $\mathbf{x}(0) = \mathbf{x}_k \in \Sigma_{m1}$. Construct a conewise linear system (33) by setting $\mu = 0$ in (2). Let Λ for the conewise linear system (33) be defined by (5), (6), (7) and (9).

The following two statements hold for the trajectories $\mathbf{x}(t)$ of the conewise affine system (2):

(i) *When $\Lambda < 1$, there exists an $\mathbf{x}_F \in \Sigma_{m1}$ such that $\|M(\mathbf{x}_k)\| < \|\mathbf{x}_k\|,\ \forall \mathbf{x}_k \in R := \{\mathbf{x} \in \Sigma_{m1} |\ \|\mathbf{x}\| \geq \|\mathbf{x}_F\|\}$.*
(ii) *When $\Lambda > 1$, there exists an $\mathbf{x}_F \in \Sigma_{m1}$ such that $\|M(\mathbf{x}_k)\| > \|\mathbf{x}_k\|,\ \forall \mathbf{x}_k \in R := \{\mathbf{x} \in \Sigma_{m1} |\ \|\mathbf{x}\| \geq \|\mathbf{x}_F\|\}$.*

Proof. An analytical expression for $\mathbf{x}_F$ is obtained as follows. The conewise affine system (2) is considered as a perturbed conewise linear system, where $\mu\mathbf{b}$ is considered as the perturbation. Using the fact that the system is globally Lipschitz, the difference between the trajectory $\mathbf{x}(t)$ of the conewise affine system and the trajectory $\tilde{\mathbf{y}}(t)$ of the conewise linear system (33) can be bounded for a given time period. A trajectory of $\tilde{\mathbf{y}}(t)$ from $\tilde{\mathbf{y}}_0 \in \Sigma_{m1}$ is studied, that encircles the origin and crosses the boundary Σ_{m1} after one spiralling motion. We will use an initial condition $\tilde{\mathbf{y}}_0$, with $\|\tilde{\mathbf{y}}_0\|$ large enough, such that the trajectories $\tilde{\mathbf{y}}(t)$ and $\mathbf{x}(t)$ emanating from this initial position will encircle the origin and traverse the boundary Σ_{m1}, independent of the direction of the bounded perturbation. To find such an initial condition $\tilde{\mathbf{y}}_0$ we first study an arbitrary initial position $\mathbf{y}_0 \in \Sigma_{m1}$, for which the trajectory $\mathbf{y}(t)$ of (33) is followed during one spiralling period.

Let T be the period time of the spiralling motion of (33), as given in [13]. Consider a trajectory $\mathbf{y}(t), t \in [0, T]$, of (33) with an arbitrary initial condition $\mathbf{y}_0 \in \Sigma_{m1} \setminus \{\mathbf{0}\}$ at time $t = 0$. From the stability analysis of the system (33), we obtain $\mathbf{y}(T) = \Lambda\mathbf{y}_0$, where Λ is defined in (5), (6), (7) and (9).

Define the open set $\mathcal{C}(\mathbf{y}_0)$ as:

$$\mathcal{C}(\mathbf{y}_0) := \begin{cases} (\mathcal{S}_m \cup \Sigma_{m1} \cup \mathcal{S}_1) \cap \{\mathbf{y} \in \mathbb{R}^2 | 0 < \mathbf{t}_{m1}^T\mathbf{y} < \|\mathbf{y}_0\|\}, & \text{if } \Lambda < 1, \\ (\mathcal{S}_m \cup \Sigma_{m1} \cup \mathcal{S}_1) \cap \{\mathbf{y} \in \mathbb{R}^2 | \mathbf{t}_{m1}^T\mathbf{y} > \|\mathbf{y}_0\|\}, & \text{if } \Lambda > 1. \end{cases} \tag{34}$$

Note that $\mathbf{t}_{m1}$ is a unit vector. The set $\mathcal{C}(\mathbf{y}_0)$ is shown in Fig. 9. Without loss of generality, assume that for all $\mathbf{y} \in \Sigma_{m1} \setminus \{\mathbf{0}\}$ the vector field $\mathbf{f}(\mathbf{y})$ of (33) is pointing in direction of $\mathcal{S}_1$. Here, no generality is lost, since $\mathbf{f}(\cdot)$ is homogeneous, $\Sigma_{m1} \setminus \{\mathbf{0}\}$ is a halfline from the origin and $\mathcal{S}_i$ can be renumbered such that $\mathbf{f}(\mathbf{y})$ is pointing in direction of $\mathcal{S}_1$ for all $\mathbf{y} \in \Sigma_{m1} \setminus \{\mathbf{0}\}$. Since $\mathbf{y}(T) \in \Sigma_{m1}$ and $\mathbf{f}(\mathbf{y}(T))$ is pointing in direction of $\mathcal{S}_1$, one can conclude that there exist small times $\tau_-, \tau_+ \in (0, T)$ such that the trajectory $\mathbf{y}(t)$ satisfies the following three conditions:

$$\mathbf{y}(t) \in \mathcal{C}(\mathbf{y}_0), \quad \forall t \in [T - \tau_-, T + \tau_+], \tag{35}$$
$$\mathbf{y}(T - \tau_-) \in \mathcal{C}(\mathbf{y}_0) \cap \mathcal{S}_m, \tag{36}$$
$$\mathbf{y}(T + \tau_+) \in \mathcal{C}(\mathbf{y}_0) \cap \mathcal{S}_1. \tag{37}$$

Here, the following facts are used; the trajectory $\mathbf{y}(t)$ is continuous in time, the point $\mathbf{y}(T) \in \mathcal{C}(\mathbf{y}_0)$ and the trajectory traverses Σ_{m1} from $\mathcal{S}_m$ towards $\mathcal{S}_1$ at the time instant $t = T$. Since $\mathcal{C}(\mathbf{y}_0)$, $\mathcal{S}_m$ and $\mathcal{S}_1$ are open sets, there exists an $\epsilon \in (0, \infty)$, such that for all vectors $\boldsymbol{\delta}$, with $\|\boldsymbol{\delta}\| \leq \epsilon$ the conditions

$$\mathbf{y}(t) + \boldsymbol{\delta} \in \mathcal{C}(\mathbf{y}_0), \quad \forall t \in [T - \tau_-, T + \tau_+], \tag{38}$$
$$\mathbf{y}(T - \tau_-) + \boldsymbol{\delta} \in \mathcal{C}(\mathbf{y}_0) \cap \mathcal{S}_m, \tag{39}$$
$$\mathbf{y}(T + \tau_+) + \boldsymbol{\delta} \in \mathcal{C}(\mathbf{y}_0) \cap \mathcal{S}_1, \tag{40}$$

are satisfied. These conditions are illustrated in Fig. 9. A new initial condition $\tilde{\mathbf{y}}_0 = k\mathbf{y}_0$, with k a positive constant, is chosen for the system (33). Application of Lemma 12 yields, that $\tilde{\mathbf{y}}(t) = k\mathbf{y}(t)$. We introduce $\boldsymbol{\zeta} = k\boldsymbol{\delta}$, such that combination of the conditions (38)-(40) with definition (34) yields:

$$\tilde{\mathbf{y}}(t) + \boldsymbol{\zeta} \in \mathcal{C}(\tilde{\mathbf{y}}_0), \quad \forall t \in [T - \tau_-, T + \tau_+], \tag{41}$$
$$\tilde{\mathbf{y}}(T + \tau_-) + \boldsymbol{\zeta} \in \mathcal{C}(\tilde{\mathbf{y}}_0) \cap \mathcal{S}_m, \tag{42}$$
$$\tilde{\mathbf{y}}(T + \tau_+) + \boldsymbol{\zeta} \in \mathcal{C}(\tilde{\mathbf{y}}_0) \cap \mathcal{S}_1, \tag{43}$$

for the trajectory $\tilde{\mathbf{y}}(t)$ with initial condition $\tilde{\mathbf{y}}_0 = k\mathbf{y}_0$ and for all $\boldsymbol{\zeta}$ with $\|\boldsymbol{\zeta}\| \leq k\epsilon$.

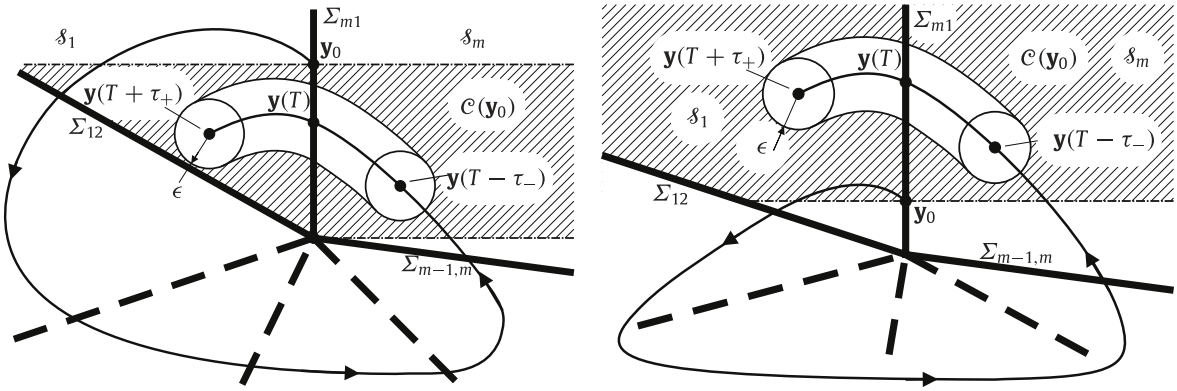

Fig. 9. Graphical representation of the conditions (38)–(40) for $\Lambda < 1$ and $\Lambda > 1$. The set $\mathcal{C}(\mathbf{y}_0)$ is shown as the dashed region. Note that the domain around $\mathbf{y}(t),\ t \in [T-\tau_-, T+\tau_+]$ is contained in $\mathcal{C}(\mathbf{y}_0)$.

Now, consider the affine term of (2), i.e. $\mu\mathbf{b}$, as a constant disturbance of the system (33). We study the trajectory $\mathbf{x}(t)$ of (2) and the trajectory $\tilde{\mathbf{y}}(t)$ of (33), both with the same initial condition $\mathbf{x}_k = \tilde{\mathbf{y}}_0 = k\mathbf{y}_0$ at $t = 0$. Since system (2) is globally Lipschitz with Lipschitz constant L, Theorem 3.4 in [17] can be applied, yielding

$$\|\tilde{\mathbf{y}}(t) - \mathbf{x}(t)\| \leq \frac{|\mu|}{L}\left(e^{L(T+\tau_+)} - 1\right), \quad \forall t \in [0, T+\tau_+], \tag{44}$$

where μ is given in (2), T the period of the spiralling motion of (33) and τ_+ is introduced above. If we choose $\tilde{\mathbf{y}}_0 \in R := \left\{\tilde{\mathbf{y}}_0 \in \mathbb{R}^2 | \tilde{\mathbf{y}}_0 = k\mathbf{y}_0,\ k \geq \frac{|\mu|}{\epsilon L}\left(e^{L(T+\tau_+)} - 1\right)\right\}$, with $\mathbf{y}_0$ and ϵ introduced above, then (44) yields $\|\mathbf{x}(t) - \tilde{\mathbf{y}}(t)\| \leq k\epsilon$, $\forall t \in [0, T+\tau_+]$ and (41)–(43) yield:

$$\mathbf{x}(t) \in \mathcal{C}(\mathbf{x}_k), \quad \forall t \in [T-\tau_-, T+\tau_+], \tag{45}$$

$$\mathbf{x}(T-\tau_-) \in \mathcal{C}(\mathbf{x}_k) \cap \mathcal{S}_m, \tag{46}$$

$$\mathbf{x}(T+\tau_+) \in \mathcal{C}(\mathbf{x}_k) \cap \mathcal{S}_1, \tag{47}$$

where we used $\mathbf{x}_k = \tilde{\mathbf{y}}_0$. From these conditions we conclude that the continuous trajectory $\mathbf{x}(t)$ of (2) crosses $\Sigma_{m1} \cap \mathcal{C}(\mathbf{x}_k)$ at a time $t_c \in (T-\tau_-, T+\tau_+)$. The definition of the map M in Lemma 13 yields $M(\mathbf{x}_k) = \mathbf{x}(t_c) \in \Sigma_{m1} \cap \mathcal{C}(\mathbf{x}_k)$, where $\mathbf{x}(t)$ denotes the trajectory of (2) with initial condition $\mathbf{x}_k$. For $\Lambda < 1$, the intersection $\Sigma_{m1} \cap \mathcal{C}(\mathbf{x}_k)$ equals $\{\mathbf{x} \in \Sigma_{m1} | \|\mathbf{x}\| \in (0, \|\mathbf{x}_k\|)\}$. For $\Lambda > 1$, the intersection $\Sigma_{m1} \cap \mathcal{C}(\mathbf{x}_k)$ equals $\{\mathbf{x} \in \Sigma_{m1} | \|\mathbf{x}\| > \|\mathbf{x}_k\|\}$.

The set R can be written as $R = \{\mathbf{x} \in \Sigma_{m1} |\ \|\mathbf{x}\| \geq \|\mathbf{x}_F\|\}$, with

$$\mathbf{x}_F := \frac{|\mu|}{\epsilon L}\left(e^{L(T+\tau_+)} - 1\right)\mathbf{y}_0, \quad \mathbf{y}_0 \in \Sigma_{m1} \setminus \{\mathbf{0}\}. \tag{48}$$

Hence, for $\Lambda < 1$, we obtain $\|M(\mathbf{x}_k)\| < \|\mathbf{x}_k\|$, $\forall \mathbf{x}_k \in R = \{\mathbf{x} \in \Sigma_{m1} |\ \|\mathbf{x}\| \geq \|\mathbf{x}_F\|\}$. For $\Lambda > 1$, we obtain $\|M(\mathbf{x}_k)\| > \|\mathbf{x}_k\|$, $\forall \mathbf{x}_k \in R = \{\mathbf{x} \in \Sigma_{m1} |\ \|\mathbf{x}\| \geq \|\mathbf{x}_F\|\}$. □

Consider a trajectory from the initial condition $\mathbf{x}_0 \in R = \{\mathbf{x} \in \Sigma_{m1} |\ \|\mathbf{x}\| \geq \|\mathbf{x}_F\|\}$, with $\mathbf{x}_F$ derived in Lemma 13, and assume $\Lambda \neq 1$. Define the return map M on Σ_{m1} according to Lemma 13, and choose $\mathbf{x}_F$ as given in that lemma. The return map of the trajectory through the point $\mathbf{x}_0$ satisfies $\|M(\mathbf{x}_0)\| \neq \|\mathbf{x}_0\|$.

It remains to be proven that the trajectory from $M(\mathbf{x}_0)$ cannot return to $\mathbf{x}_0$. Without loss of generality, suppose the trajectory traverses Σ_{m1} from $\mathcal{S}_m$ towards $\mathcal{S}_1$ at $t = 0$. The vector field (2) on the boundary Σ_{m1} can be described by $\dot{\mathbf{x}} = A_1\mathbf{x} + \mu\mathbf{b},\ \mathbf{x} \in \Sigma_{m1}$, which is autonomous and affine. Hence, all trajectories traversing $[\mathbf{x}_0, M(\mathbf{x}_0)]$ cross this line from $\mathcal{S}_m$ to $\mathcal{S}_1$. Since the trajectory from $M(\mathbf{x}_0)$ cannot cross his own trajectory or $[\mathbf{x}_0, M(\mathbf{x}_0)]$, it cannot return to $\mathbf{x}_0$. No closed orbit can exist that contains a point $\mathbf{x}_0 \in R$. □

Proof of Theorem 9. Consider a visible eigenvector $\mathbf{v} \in \bar{\mathcal{S}}_i,\ i = 1, \ldots, m$, corresponding to the real eigenvalue λ_u of a system matrix A_i. Define a unit vector $\mathbf{n}_{i,i+1}$ normal to the boundary $\Sigma_{i,i+1}$ and a unit vector $\mathbf{n}_{i-1,i}$ normal to the boundary $\Sigma_{i-1,i}$, where both vectors point towards $\mathcal{S}_i$. This implies that $\mathcal{S}_i = \{\mathbf{x} \in \mathbb{R}^2 | \mathbf{x}^T\mathbf{n}_{i,i+1} > 0 \wedge \mathbf{x}^T\mathbf{n}_{i-1,i} > 0\}$.

Now, we will prove that there exists a scalar $c_H \in [0, \infty)$, such that the halfline $H = \{\mathbf{x} \in \mathbb{R}^2 | \mathbf{x} = -\mu A_i^{-1}\mathbf{b} + c\mathbf{v}, c \in [c_H, \infty)\}$ is included completely in $\bar{\mathcal{S}}_i$, the closure of $\mathcal{S}_i$. Taking the inner product of the vectors $\mathbf{x} = -\mu A_i^{-1}\mathbf{b} + c\mathbf{v}$, $c \in (0, \infty)$ with $\mathbf{n}_{i-1,i}$ and $\mathbf{n}_{i,i+1}$, we find that $\mathbf{x}^T\mathbf{n}_{i-1,i} > 0$ if $c > \frac{\mu\mathbf{n}_{i-1,i}^T A_i^{-1}\mathbf{b}}{\mathbf{n}_{i-1,i}^T\mathbf{v}}$ and $\mathbf{x}^T\mathbf{n}_{i,i+1} > 0$ if $c > \frac{\mu\mathbf{n}_{i,i+1}^T A_i^{-1}\mathbf{b}}{\mathbf{n}_{i,i+1}^T\mathbf{v}}$. Both denominators are

nonzero and positive, since the visible eigenvector $\mathbf{v}$ is not contained in either of the boundaries $\Sigma_{i-1,i}$ or $\Sigma_{i,i+1}$ and $\mathbf{v} \in \bar{\mathcal{S}}_i$ according to Definition 2. The set H is contained in the closure of $\mathcal{S}_i$, i.e. $H \subset \bar{\mathcal{S}}_i$, when $c_H = \max(\frac{\mu \mathbf{n}_{i-1,i}^T A_i^{-1}\mathbf{b}}{\mathbf{n}_{i-1,i}^T \mathbf{v}}, \frac{\mu \mathbf{n}_{i,i+1}^T A_i^{-1}\mathbf{b}}{\mathbf{n}_{i,i+1}^T \mathbf{v}})$.

Consider a trajectory of (2) with initial position $\mathbf{x}_0 \in H$. Any position in H can be written as $\mathbf{x} = -\mu A_i^{-1}\mathbf{b} + c\mathbf{v}$, such that substitution in (2) yields $\dot{\mathbf{x}} = cA_i\mathbf{v}$. However, since $\mathbf{v}$ is an eigenvector, we obtain $\dot{\mathbf{x}} = c\lambda_u\mathbf{v}$. This vector field is tangent to the halfline H. This implies, that trajectories can only enter or leave the halfline H at $\mathbf{x} = -\mu A_i^{-1}\mathbf{b} + c_H\mathbf{v}$, the end point of the halfline. When the vector field at this point is into (out of) H, then H is a positively (negatively) invariant set.

Uniqueness of solutions of (2) excludes closed orbits inside the halfline H. In addition, a closed orbit cannot traverse H, since in that case, the closed orbit should enter and leave H. This is not possible, since H is either a positively or negatively invariant set. No closed orbits can exist that either are contained in H, or contain a point in H. □

Proof of Theorem 10. The proof of this theorem is given in two parts. In Part 1, the theorem is proven for all $\nu \in N \setminus \{0\}$. Subsequently, in Part 2, the case $\nu = 0$ is discussed.

Part 1

In this part we will first discuss the existence of equilibria for $\nu \neq 0$, subsequently their local stability properties are discussed. Let $J \subseteq \{1, \ldots, \bar{m}\}$ contain the indices, such that the domains $\bar{\mathcal{D}}_i$, $i \in J$ contain the origin. According to Assumption 1, $\mathbf{F}_i(\mathbf{0}, 0) = \mathbf{0}$, $\forall i \in J$. With Assumption 4, we can apply the Implicit Function Theorem, cf. [21], which yields that for each $i \in J$ locally there exists a smooth path $\mathbf{x}_{i,1}(\nu)$, that satisfies $\mathbf{F}_i(\mathbf{x}_{i,1}(\nu), \nu) = \mathbf{0}$. Note that this path may be positioned outside $\bar{\mathcal{D}}_i$. When $\mathbf{x}_{i,1}(\nu) \in \bar{\mathcal{D}}_i$ for given $\nu \in N$, then an equilibrium of (1) exists in this domain. Assumption 5 excludes the possibility that there exists an equilibrium in the domain $\bar{\mathcal{D}}_i$ for $\nu \in N$ when $\mathcal{D}_i$ is a cusp-shaped region at the origin. (Note that a cusp-shaped region is not represented by a cone in (2)). Therefore, we may restrict ourselves to the paths of possible equilibria $\mathbf{x}_{i,1}(\nu)$, $i \in \{1, \ldots, m\} \subseteq J$.

Differentiating $\mathbf{F}_i(\mathbf{x}_{i,1}(\nu), \nu) = \mathbf{0}$ with respect to ν, we obtain with Assumptions 2 and 4:

$$\left.\frac{\partial \mathbf{F}_i}{\partial \nu}\right|_{(\mathbf{x},\nu)=(\mathbf{0},0)} + \left.\frac{\partial \mathbf{F}_i}{\partial \mathbf{x}}\right|_{(\mathbf{x},\nu)=(\mathbf{0},0)} \left.\frac{\partial \mathbf{x}_{i,1}(\nu)}{\partial \nu}\right|_{(\mathbf{x},\nu)=(\mathbf{0},0)} = \mathbf{0},$$

$$\left.\frac{\partial \mathbf{x}_{i,1}(\nu)}{\partial \nu}\right|_{(\mathbf{x},\nu)=(\mathbf{0},0)} = -A_i^{-1}\mathbf{b}. \tag{49}$$

To prove the first statement of the theorem for $\nu, \mu \neq 0$, without loss of generality we may assume there exists a positive ν^*, such that $\mathbf{x}_{i,1}(\nu) \in \mathcal{D}_i$ for all $\nu \in (0, \nu^*)$ for a given $i \in \{1, \ldots, m\}$, where an open set $\mathcal{D}_i$ is chosen since we adopted Assumption 5. This implies that $\left.\frac{\partial \mathbf{x}_{i,1}(\nu)}{\partial \nu}\right|_{(\mathbf{x},\nu)=(\mathbf{0},0)} = -A_i^{-1}\mathbf{b} \in \mathcal{D}_i$, and since $\mathcal{D}_i$ is locally approximated by $\mathcal{S}_i$ and $\mu = \nu > 0$, we obtain $-\mu A_i^{-1}\mathbf{b} \in \mathcal{S}_i$, for $\mu > 0$. In combination with the fact that equilibria of (2) are positioned on $\mathbf{x}_{i,2}(\mu) = -\mu A_i^{-1}\mathbf{b}$, we obtain the following result: when (1) contains an equilibrium in $\mathcal{D}_i$ for an $i \in \{1, \ldots, m\}$ and ν in a range $(0, \nu^*)$, then (2) contains an equilibrium point in $\mathcal{S}_i$ for all $\mu > 0$.

To prove the converse statement, we note that with Assumption 5, all paths of equilibria of (2) will be positioned in a cone $\mathcal{S}_i$, $i = 1, \ldots, m$. Therefore, we assume without loss of generality that (2) contains an equilibrium path $\mathbf{x}_{i,2}(\mu) \in \mathcal{S}_i$ for $\mu > 0$ and given $i \in \{1, \ldots, m\}$, such that $\mathbf{f}_i(\mathbf{x}_{i,2}(\mu), \mu) = \mathbf{0}$. Solving this equation yields $\mathbf{x}_{i,2}(\mu) = -\mu A_i^{-1}\mathbf{b} \in \mathcal{S}_i$, $\forall \mu > 0$. Using (49), we obtain: $\left.\frac{\partial \mathbf{x}_{i,1}(\nu)}{\partial \nu}\right|_{(\mathbf{x},\nu)=(\mathbf{0},0)} \in \mathcal{S}_i$, where $\mathbf{x}_{i,1}(\nu)$ denotes a path such that $\mathbf{F}_i(\mathbf{x}_{i,1}(\nu), \nu) = \mathbf{0}$ holds. The domain $\mathcal{D}_i$ is locally approximated by $\mathcal{S}_i$, such that we have: $\left.\frac{\partial \mathbf{x}_{i,1}(\nu)}{\partial \nu}\right|_{(\mathbf{x},\nu)=(\mathbf{0},0)} \in \mathcal{D}_i$. Since $\mathbf{x}_{i,1}(\nu)$ is a smooth path and $\mathcal{D}_i$ is an open set, therefore there exists a $\nu^* > 0$ such that $\mathbf{x}_{i,1}(\mu) \in \mathcal{D}_i$, $\forall \nu \in (0, \nu^*)$.

For $\nu, \mu \neq 0$, the final statement of Theorem 10 is obtained from the Andronov–Pontryagin condition; cf. Theorem 2.5 of [22]. Without loss of generality, we assume there exists an equilibrium of (1), that follows an equilibrium path $\mathbf{x}_{i,1}(\nu) \in \mathcal{D}_i$ for $\nu \in (0, \nu^*) \subset \bar{N}$, $\nu^* > 0$ with $i \in \{1, \ldots, m\}$. We define $\bar{\mathbf{F}}_i(\mathbf{x}, \nu) := \mathbf{F}_i(\mathbf{x} - \mathbf{x}_{i,1}(\nu), \nu)$ for $\nu \in (0, \nu^*)$, which is a smooth function, such that $\dot{\mathbf{x}} = \bar{\mathbf{F}}_i(\mathbf{x}, \nu)$ describes the dynamics of (1) in a neighbourhood $M(\nu)$ near the equilibrium. For each $\nu \in (0, \nu^*)$, $M(\nu) \ni \mathbf{0}$ is chosen such, that for all $\hat{\mathbf{x}} \in M(\nu)$, $\hat{\mathbf{x}} + \mathbf{x}_{i,1}(\nu)$ lies inside $\mathcal{D}_i$.

According to the Andronov–Pontryagin condition the system $\dot{\mathbf{x}} = \bar{\mathbf{F}}_i(\mathbf{x}, \nu)$ is structurally stable in $M(\nu)$. Therefore, there exists an $\epsilon > 0$ such that for all vector fields $\mathbf{G}_i$ that satisfy

$$\sup_{\mathbf{x} \in M(\nu)} \left(\|\bar{\mathbf{F}}_i(\mathbf{x}) - \mathbf{G}_i(\mathbf{x})\| + \left\| \frac{\partial \bar{\mathbf{F}}_i}{\partial \mathbf{x}} - \frac{\partial \mathbf{G}_i}{\partial \mathbf{x}} \right\| \right) \leq \epsilon, \tag{50}$$

the systems $\dot{\mathbf{x}} = \mathbf{G}_i(\mathbf{x})$ and $\dot{\mathbf{x}} = \bar{\mathbf{F}}_i(\mathbf{x})$ are topologically equivalent. Choosing $\mathbf{G}_i(\mathbf{x}) = A_i\mathbf{x}$, and observing that $\bar{\mathbf{F}}_i(\mathbf{x}, \nu)$ and $\mathbf{x}_{i,1}(\nu)$ are smooth functions satisfying $\bar{\mathbf{F}}_i(\mathbf{0}, \nu) = 0$, $\mathbf{x}_{i,1}(0) = \mathbf{0}$ and $\left.\frac{\partial \bar{\mathbf{F}}_i}{\partial \mathbf{x}}\right|_{(\mathbf{x},\nu)=(\mathbf{0},0)} = \left.\frac{\partial \mathbf{G}_i}{\partial \mathbf{x}}\right|_{(\mathbf{x},\nu)=(\mathbf{0},0)} = A_i$, we can choose ν and $M(\nu)$ small enough such that (50) is satisfied. Since $\dot{\mathbf{x}} = \mathbf{G}_i(\mathbf{x})$ describes the dynamics in the neighbourhood of an equilibrium of (2), the systems (1) and (2) near their equilibria are locally topologically equivalent for $\nu \in (0, \nu^*)$ when ν^*

is chosen small enough. In addition, the stability properties of the equilibria of (2) and (1) are equal. Hence, the theorem is proven for the case $\nu \neq 0$.

Part 2

In this part, we will prove the theorem for the case $\nu = 0$. Existence of an isolated equilibrium at the origin of (1) for $\nu = 0$ is given by Assumption 1. By construction, an equilibrium at the origin exist in (2) for $\mu = 0$, which is isolated since all matrices A_i are invertible; cf. Assumption 4. It remains to be proven that the local stability properties of the equilibrium at the origin of (1) with $\nu = 0$ and (2) with $\mu = 0$ are equal.

By Assumption 4, either all trajectories near an equilibrium of (1) encircle this point, or a stable or unstable manifold of this equilibrium exist. Therefore, we will study both cases, yielding Lemmas 14 and 15, respectively.

We study manifolds of the nonsmooth systems (1) and (2) similar to the stable and unstable manifolds of nodes and saddle points in smooth dynamical systems. However, we allow these manifolds to be defined only in a domain $\bar{\mathcal{S}}_i,\ i = 1, \ldots, m$ or $\bar{\mathcal{D}}_i, i = 1, \ldots, \bar{m}$.

Lemma 14. *Under Assumptions 1 and 4, the equilibrium at the origin of (1) with $\nu = 0$ has a stable (unstable) manifold if and only if the equilibrium at the origin of (2) with $\mu = 0$ has a stable (unstable) manifold, that is tangent to the manifold of (1) at the origin.*

Proof. First, we will prove the necessity part of the lemma. By Assumption 1, an equilibrium exists at the origin for the nonsmooth system (1). Assume this equilibrium of (1) has a stable (unstable) manifold C that emanates from the origin towards a domain $\bar{\mathcal{D}}_i, i = 1, \ldots, \bar{m}$. We distinguish two cases. In Case I, we will prove that this manifold of (1) is represented in (2) when the manifold emanates from the origin towards a domain $\bar{\mathcal{D}}_i,\ i = 1, \ldots, m$, that does not form a cusp. Subsequently, we will prove this statement when the manifold emanates into a cusp-shaped domain $\bar{\mathcal{D}}_n,\ n \in \{m+1, \ldots, \bar{m}\}$ in case II.

To prove necessity in Case I, we assume that the manifold $C \in \bar{\mathcal{D}}_i,\ i = 1, \ldots, m$, is not positioned in a cusp of boundaries near the origin. Then the domain $\bar{\mathcal{D}}_i$ in (1) is represented by the cone $\bar{\mathcal{S}}_i$ in (2). When C is emanating tangentially to a boundary $\mathcal{C}_{ij}$ of (1), then we choose the index i such that on the intersection of the manifold C with a neighbourhood of the origin, the dynamics of system (1) is described by $\dot{\mathbf{x}} = \mathbf{F}_i(\mathbf{x}, 0)$. This implies that there exists a λ such that $\left.\frac{\partial \mathbf{F}_i}{\partial \mathbf{x}}\right|_{(\mathbf{x},\nu)=(\mathbf{0},0)} \mathbf{r} = \lambda \mathbf{r}$, where $\mathbf{r}$ is the vector tangent to C at the origin, with the direction chosen to satisfy $\mathbf{r} \in \bar{\mathcal{D}}_i$. Note that $\lambda < 0$ ($\lambda > 0$) for the stable (unstable) manifold. Since A_i is defined as $\left.\frac{\partial \mathbf{F}_i}{\partial \mathbf{x}}\right|_{(\mathbf{x},\nu)=(\mathbf{0},0)}$, A_i therefore has eigenvector $\mathbf{r}$. Since $\bar{\mathcal{D}}_i$ is locally approximated with $\bar{\mathcal{S}}_i$, the eigenvector $\mathbf{r}$ is visible in $\bar{\mathcal{S}}_i$. This implies that the set $c := \{\mathbf{x} \in \mathbb{R}^2 : \mathbf{x} = s\mathbf{r},\ s \in [0, \infty)\}$ is a manifold of the conewise affine system (2), on which the dynamics is given by $\dot{\mathbf{x}} = A_i\mathbf{x} = \lambda\mathbf{x}$, such that a stable (unstable) manifold of (2) corresponds to a stable (unstable) manifold of (1).

To prove necessity in Case II, we assume that the manifold C is emanating from the origin towards a cusp of boundaries into a domain $\mathcal{D}_n,\ n \in \{m+1, \ldots, \bar{m}\}$ of (1), and $\mathbf{r}$ is the vector pointing into this cusp from the origin, then there exists a λ such that $\left.\frac{\partial \mathbf{F}_n}{\partial \mathbf{x}}\right|_{(\mathbf{x},\nu)=(\mathbf{0},0)} \mathbf{r} = \lambda \mathbf{r}$. Without loss of generality, we assume that we do not have two or more adjoining cusp-shaped regions. Note that $\lambda < 0$ ($\lambda > 0$) for the stable (unstable) manifold. Since the vector field of (1) is continuous at each boundary $\mathcal{C}_{ij}$, we observe that $\frac{\partial \mathbf{F}_i}{\partial \mathbf{x}} \mathbf{t}_{\mathcal{C}_{ij}}(\mathbf{x}) = \frac{\partial \mathbf{F}_j}{\partial \mathbf{x}} \mathbf{t}_{\mathcal{C}_{ij}}(\mathbf{x}), \forall \mathbf{x} \in \mathcal{C}_{ij}$, where $\mathbf{t}_{\mathcal{C}_{ij}}(\mathbf{x})$ denotes a vector tangent to $\mathcal{C}_{ij}$ at the point $\mathbf{x}$. Therefore, $\left.\frac{\partial \mathbf{F}_n}{\partial \mathbf{x}}\right|_{(\mathbf{x},\nu)=(\mathbf{0},0)} \mathbf{r} = \lambda \mathbf{r}$ implies that $\left.\frac{\partial \mathbf{F}_i}{\partial \mathbf{x}}\right|_{(\mathbf{x},\nu)=(\mathbf{0},0)} \mathbf{r} = \left.\frac{\partial \mathbf{F}_j}{\partial \mathbf{x}}\right|_{(\mathbf{x},\nu)=(\mathbf{0},0)} \mathbf{r} = \lambda \mathbf{r}$, with the indices $i, j \in \{1, \ldots m\}$ chosen such that the domains $\mathcal{D}_i$ and $\mathcal{D}_j$ have boundaries tangent to the cusp at the origin, although the domains $\mathcal{D}_i$ and $\mathcal{D}_j$ do not form a cusp at the origin. Since A_i and A_j are, respectively, defined as $\left.\frac{\partial \mathbf{F}_i}{\partial \mathbf{x}}\right|_{(\mathbf{x},\nu)=(\mathbf{0},0)}$ and $\left.\frac{\partial \mathbf{F}_j}{\partial \mathbf{x}}\right|_{(\mathbf{x},\nu)=(\mathbf{0},0)}$, both A_i and A_j have eigenvector $\mathbf{r}$. The domains $\bar{\mathcal{D}}_i$ and $\bar{\mathcal{D}}_j$ are locally approximated with, respectively, $\bar{\mathcal{S}}_i$ and $\bar{\mathcal{S}}_j$, such that the eigenvector $\mathbf{r}$ is visible and lies on the boundary Σ_{ij} between $\mathcal{S}_i$ and $\mathcal{S}_j$. This implies that the set $c := \{\mathbf{x} \in \mathbb{R}^2 : \mathbf{x} = s\mathbf{r},\ s \in [0, \infty)\}$ is a manifold of the conewise affine system (2), on which the dynamics is given by $\dot{\mathbf{x}} = A_i\mathbf{x} = A_j\mathbf{x} = \lambda\mathbf{x}$, such that a stable (unstable) manifold of (2) corresponds to the stable (unstable) manifold of (1). In both cases, the necessity part of the lemma is obtained.

Now, we will prove the sufficiency part of the lemma by assuming that there exists a stable (unstable) manifold $c \in \bar{\mathcal{S}}_i,\ i = 1, \ldots, m$, of the system (2). By Lemma 12, we can denote this manifold with $c = \{\mathbf{x} \in \mathbb{R}^2 : \mathbf{x} = s\mathbf{r},\ s \in [0, \infty)\}$, where $\mathbf{r} \in \bar{\mathcal{S}}_i$ is an eigenvector of A_i. Let λ be the eigenvalue corresponding to this eigenvector. Since c is a stable (unstable) manifold, we obtain $\lambda < 0$ ($\lambda > 0$). Again, two cases are distinguished. First, we will study the case where c is positioned in an open cone $\mathcal{S}_i$, subsequently we will prove the sufficiency part of the theorem in case c is positioned on a boundary.

To prove sufficiency in the first case, we assume that the stable (unstable) manifold c is positioned in an open cone $\mathcal{S}_i$. Then the Hartman–Grobman Theorem, [10], guarantees that the system $\dot{\mathbf{x}} = \mathbf{F}_i(\mathbf{x}, 0)$ locally has the same stable and unstable manifolds as the system $\dot{\mathbf{x}} = A_i\mathbf{x}$. Therefore, the vector field $\mathbf{F}_i(\mathbf{x}, 0)$ satisfies $\left.\frac{\partial \mathbf{F}_i}{\partial \mathbf{x}}\right|_{(\mathbf{x},\nu)=(\mathbf{0},0)} \mathbf{r} = \lambda \mathbf{r}$. Since the trajectories of (2) in the cone $\bar{\mathcal{S}}_i$ coincide with the trajectories of $\dot{\mathbf{x}} = A_i\mathbf{x}$ and the trajectories of (1) in the domain $\bar{\mathcal{D}}_i$ coincide with the trajectories of $\dot{\mathbf{x}} = \mathbf{F}_i(\mathbf{x}, 0)$, the nonsmooth system (1) has a stable (unstable) manifold corresponding to c if $\lambda < 0$ ($\lambda > 0$).

To prove sufficiency in the second case, we assume the stable (unstable) manifold c of (2) lies on a boundary Σ_{ij}. Recall that $\mathbf{t}_{ij}$ denotes the vector tangent to Σ_{ij}, pointing towards this ray. Let $K \subseteq \{1, \ldots, \bar{m}\}$ denote the set of indices, such that $\bar{\mathcal{D}}_n$ has a boundary tangent to Σ_{ij} at the origin if and only if $n \in K$. (The domain $\bar{\mathcal{D}}_n$ may or may not be a cusp-shaped region).

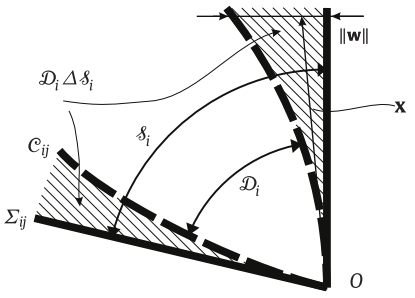

Fig. 10. Schematic representation of the set $\mathcal{D}_i \Delta \mathcal{S}_i$, depicted shaded, that consists of two parts, where $\|\mathbf{w}\|$ is locally quadratic in $\|\mathbf{x}\|$.

We assumed the existence of a stable (unstable) manifold c of (2) on a boundary Σ_{ij}. This implies that there exists a $\lambda < 0$ ($\lambda > 0$) such that $A_i \mathbf{t}_{ij} = \lambda \mathbf{t}_{ij} = \frac{\partial \mathbf{F}_i}{\partial \mathbf{x}}\Big|_{(\mathbf{x},\nu)=(\mathbf{0},0)} \mathbf{t}_{ij}$. For the sake of contradiction, suppose (1) has no stable (unstable) manifold tangent to Σ_{ij}. Then $\forall n \in K, \forall \lambda_n < 0$ ($\lambda_n > 0$) : $\frac{\partial \mathbf{F}_n}{\partial \mathbf{x}}\Big|_{(\mathbf{x},\nu)=(\mathbf{0},0)} \mathbf{t}_{ij} \neq \lambda_n \mathbf{t}_{ij}$. However, since $\mathbf{F}(\mathbf{x}, \nu)$ is continuous, we obtain $\frac{\partial \mathbf{F}_i}{\partial \mathbf{x}}\Big|_{(\mathbf{x},\nu)=(\mathbf{0},0)} \mathbf{t}_{ij} = \frac{\partial \mathbf{F}_n}{\partial \mathbf{x}}\Big|_{(\mathbf{x},\nu)=(\mathbf{0},0)} \mathbf{t}_{ij}$, $\forall n \in K$. Hence, $A_i = \frac{\partial \mathbf{F}_i}{\partial \mathbf{x}}\Big|_{(\mathbf{x},\nu)=(\mathbf{0},0)}$ has no eigenvalue $\lambda < 0, (\lambda > 0)$ with the eigenvector $\mathbf{t}_{ij}$, contradicting the existence of a stable (unstable) manifold with eigenvalue λ in (2). A contradiction is obtained, such that (1) has a stable (unstable) manifold, which is tangent to Σ_{ij} at the equilibrium. In both cases, the sufficiency part of the lemma is proven. □

Lemma 15. *Under Assumptions 1, 4 and 6, all trajectories of (1) with $\nu = 0$ in a neighbourhood around the equilibrium at the origin are spiralling around the origin and converge towards the origin for $t \to \infty$ ($t \to -\infty$) if and only if all trajectories of (2) with $\mu = 0$ are spiralling around the origin and converge to the origin for $t \to \infty$ ($t \to -\infty$).*

Proof. First we prove the sufficiency part of the statement, subsequently the necessity part of the statement is proven. Assume a spiralling motion exists in the system (2). Since system (2) is Lipschitz continuous, the time-reversed system can be studied, and the chosen coordinate frame may be mirrored along a coordinate axis we may assume, without loss of generality, that the spiralling motion is counter clockwise and trajectories of (2) are converging to the origin for $t \to \infty$. We consider a trajectory of (2) starting at $t = 0$ from a point $\mathbf{x}_0$ which is positioned on the positive vertical axis. There exists a time T such that the trajectory $\mathbf{x}(t)$ of (2) encircles the origin O once and returns to a point $\mathbf{x}(T)$ on the interval of the line segment $[O, \mathbf{x}_0]$. We will compare the trajectories $\mathbf{x}(t)$ of (2) with $\tilde{\mathbf{x}}(t)$ of (1), where both are starting from $\mathbf{x}(0) = \tilde{\mathbf{x}}(0) = \mathbf{x}_0$. With the same reasoning as used in the proof of Theorem 8, we can find finite $\tau, E > 0$, such that $\tilde{\mathbf{x}}(t)$ traverses the interior of $[O, \mathbf{x}_0]$ at a time $t_c \in (T - \tau, T + \tau)$ if $\|\mathbf{x}(t) - \tilde{\mathbf{x}}(t)\| \leq E, \forall t \in [0, T + \tau]$. Let L be a Lipschitz constant of both $\mathbf{F}(\mathbf{x}, 0)$, given in (1) and $\mathbf{f}(\mathbf{x}, 0)$, given in (2). Theorem 3.4 of [17] guarantees that the requirement $\|\mathbf{x}(t) - \tilde{\mathbf{x}}(t)\| \leq E, \forall t \in [0, T + \tau]$ is met when $\|\mathbf{F}(\mathbf{x}, 0) - \mathbf{f}(\mathbf{x}, 0)\| < D := \frac{LE}{e^{L(T+\tau)} - 1}$, $\forall \mathbf{x} \in R(\mathbf{x}_0)$, where the open, bounded set $R(\mathbf{x}_0)$ is chosen such that the previously mentioned trajectories satisfy $\mathbf{x}(t), \tilde{\mathbf{x}}(t) \in R(\mathbf{x}_0), \forall t \in [0, T + \tau]$. Next, we will prove that, by choosing $\mathbf{x}_0$ small, $\|\mathbf{F}(\mathbf{x}, 0) - \mathbf{f}(\mathbf{x}, 0)\| < D$ holds for all $\mathbf{x} \in R(\mathbf{x}_0)$.

From Lemma 12, we find that trajectories of the conewise affine system with $\mu = 0$ scale linearly with initial conditions, such that E and $R(\mathbf{x}_0)$ can be chosen such that they scale linearly with $\|\mathbf{x}_0\|$. We will prove that $\|\mathbf{F}(\mathbf{x}, 0) - \mathbf{f}(\mathbf{x}, 0)\| = \mathcal{O}(L\|\mathbf{x}\|^2, \|\mathbf{x}\|^2)$, such that by decreasing $\|\mathbf{x}_0\|$, $\|\mathbf{F}(\mathbf{x}, 0) - \mathbf{f}(\mathbf{x}, 0)\| < D$, $\forall \mathbf{x} \in R(\mathbf{x}_0)$ can be satisfied. By the Taylor expansion of $\mathbf{F}_i(\mathbf{x}, 0)$, we obtain:

$$\|\mathbf{F}_i(\mathbf{x}, 0) - \mathbf{f}_i(\mathbf{x}, 0)\| = \mathcal{O}(\|\mathbf{x}\|^2). \tag{51}$$

Define $\mathcal{D}_i \Delta \mathcal{S}_i := (\mathcal{D}_i \cup \mathcal{S}_i) \setminus (\mathcal{D}_i \cap \mathcal{S}_i)$, which is given in Fig. 10. The width $\|\mathbf{w}\|$ of this set, as graphically defined in Fig. 10, is locally quadratic with $\|\mathbf{x}\|$. Since on one of the boundaries of $\mathcal{D}_i \Delta \mathcal{S}_i$, the dynamics is described by $\dot{\mathbf{x}} = \mathbf{F}_i(\mathbf{x}, 0)$, we apply the Lipschitz property of (1) to obtain:

$$\|\mathbf{F}(\mathbf{x}, 0) - \mathbf{F}_i(\mathbf{x}, 0)\| = \mathcal{O}(L\|\mathbf{x}\|^2), \quad \forall \mathbf{x} \in \mathcal{D}_i \Delta \mathcal{S}_i. \tag{52}$$

Combination of (51) with (52) yields:

$$\|\mathbf{F}(\mathbf{x}, 0) - \mathbf{f}_i(\mathbf{x}, 0)\| = \mathcal{O}(L\|\mathbf{x}\|^2, \|\mathbf{x}\|^2), \quad \forall \mathbf{x} \in \mathcal{D}_i \Delta \mathcal{S}_i \cup (\mathcal{D}_i \cap \mathcal{S}_i), \tag{53}$$

such that we obtain

$$\|\mathbf{F}(\mathbf{x}, 0) - \mathbf{f}(\mathbf{x}, 0)\| = \mathcal{O}(L\|\mathbf{x}\|^2, \|\mathbf{x}\|^2), \quad \forall \mathbf{x} \in \mathbb{R}^2. \tag{54}$$

By choosing $\mathbf{x}_0$ small enough, $R(\mathbf{x}_0)$ becomes small enough, such that $\|\mathbf{F}(\mathbf{x}, 0) - \mathbf{f}(\mathbf{x}, 0)\| < D$, $\mathbf{x} \in R(\mathbf{x}_0)$. Given this set $R(\mathbf{x}_0)$, we conclude that the trajectory $\tilde{\mathbf{x}}(t)$ from $\mathbf{x}_0 \in R(\mathbf{x}_0)$, starting from the positive vertical axis, crosses the interior of

the line $[O, \mathbf{x}_0]$ in the time interval $[T-\tau, T+\tau]$. Consequently, the nonsmooth system (1) exhibits a spiralling motion, and trajectories of (1) in the neighbourhood $R(\mathbf{x}_0)$ do converge to the origin for $t \to \infty$, when $\|\mathbf{x}_0\|$ is chosen small enough.

The necessity part of the statement is equivalent with the statement that the absence of a stable (unstable) spiralling motion of (2) with $\mu = 0$ excludes a stable (unstable) spiralling motion of (1) with $\nu = 0$. To prove the latter statement, assume the conewise linear system (2) with $\mu = 0$ does not exhibit spiralling motion, converging to the origin for $t \to \infty$ ($t \to -\infty$). Considering Assumptions 4 and 6, system (2) should either exhibit spiralling motion converging to the origin for $t \to -\infty$ ($t \to \infty$), or should contain visible eigenvectors. In the first case, the spiralling motion, converging to the origin for $t \to -\infty$ ($t \to \infty$), implies that in a neighbourhood of R of the origin, a spiralling motion of (1) with $\nu = 0$ exist, and trajectories converge to the origin for $t \to -\infty$ ($t \to \infty$). This follows directly from the sufficiency part of the proof. In case visible eigenvectors exist in (2) with $\mu = 0$, Lemma 14 guarantees that a manifold exist in (1) for $\nu = 0$, emanating from the origin. This manifold excludes a spiralling motion of (1) for $\nu = 0$. Hence, we have proven that the absence of a stable (unstable) spiralling motion of (2) with $\mu = 0$ excludes a stable (unstable) spiralling motion of (1) with $\nu = 0$. □

Given Assumption 4 an equilibrium is unstable when either an unstable manifold exist, or a diverging spiralling motion occurs. An equilibrium point is locally asymptotically stable, when a converging spiralling motion exist or when a stable manifold exist, and no unstable manifolds. Trajectories encircling an equilibrium, which are not converging to this point for $t \to \infty$ or $t \to -\infty$, are, in a neighbourhood around the origin, excluded by Assumption 6. Therefore, application of Lemma 14 guarantees that at $\nu = \mu = 0$, the stability properties of the equilibrium at the origin of (1) and (2) are equal when visible eigenvectors exist in (1). When no visible eigenvectors exist in (1), then the stability properties of the equilibria at the origin of (1) and (2) are equal according to Lemma 15. □

Proof of Theorem 11. To prove Theorem 11, first we will introduce a new coordinate system, and derive the technical Lemma 16 for the obtained system. Subsequently, in Lemma 17 we will state an intermediate result about the number of limit cycles, which will be used to prove the theorem.

In a new coordinate system $\mathbf{z} = \frac{\mathbf{x}}{\mu}$, defined for $\mu \neq 0$, the conewise affine system (2) is represented as:

$$\begin{aligned} &\dot{\mathbf{z}} = \tilde{\mathbf{f}}(\mathbf{z}), \\ &\tilde{\mathbf{f}}(\mathbf{z}) = A_i\mathbf{z} + \mathbf{b}, \quad \mathbf{z} \in \mathcal{S}_i. \end{aligned} \tag{55}$$

Clearly, this transformation does not change the existence and stability of limit sets of the conewise affine system. Expressing (1) in the coordinates $\mathbf{z} = \frac{\mathbf{x}}{\nu}$, defined for $\nu \neq 0$, we obtain:

$$\begin{aligned} &\dot{\mathbf{z}} = \tilde{\mathbf{F}}(\mathbf{z}, \nu), \\ &\tilde{\mathbf{F}}(\mathbf{z}, \nu) = \tilde{\mathbf{F}}_i(\mathbf{z}, \nu) := \frac{1}{\nu}\mathbf{F}_i(\nu\mathbf{z}, \nu), \quad \mathbf{z} \in \tilde{\mathcal{D}}_i, \end{aligned} \tag{56}$$

where $\tilde{\mathcal{D}}_i := \{\mathbf{z} \in \mathbb{R}^2 | \mathbf{z} = \frac{\mathbf{x}}{\nu},\ \mathbf{x} \in \mathcal{D}_i\}$.

For the difference between (55) and (56), we obtain:

Lemma 16. *Consider $\tilde{\mathbf{F}}(\mathbf{z}, \nu)$ as given in (56) and $\tilde{\mathbf{f}}(\mathbf{z})$ as given in (55). For every domain $R(\nu) := \{\mathbf{z} \in \mathbb{R}^2 | \|\mathbf{z}\| \leq c|\nu|, c > 0\}$, and for all $D > 0$ there exists a $\bar{\nu} > 0$, such that*

$$\|\tilde{\mathbf{F}}(\mathbf{z}, \nu) - \tilde{\mathbf{f}}(\mathbf{z})\| \leq D, \quad \forall \nu \in (-\bar{\nu}, \bar{\nu}),\ \forall \mathbf{z} \in R(\nu). \tag{57}$$

Proof. We observe that

$$\|\tilde{\mathbf{F}}_i(\mathbf{z}, \nu) - \tilde{\mathbf{f}}_i(\mathbf{z})\| = \frac{1}{\nu}\mathcal{O}(\nu^2\|\mathbf{z}\|^2, \nu^2\|\mathbf{z}\|, \nu^2), \tag{58}$$

$$= \mathcal{O}(\nu^3 c^2, \nu^2 c, \nu), \quad \forall \mathbf{z} \in R(\nu), \tag{59}$$

since $\mathbf{f}_i$ is a first-order approximation of $\mathbf{F}_i$, such that $\|\mathbf{F}_i(\mathbf{x}, \nu) - \mathbf{f}_i(\mathbf{x}, \nu)\| = \mathcal{O}(\|\mathbf{x}\|^2, \nu\|\mathbf{x}\|, \nu^2)$.

The set $\mathcal{D}_i \Delta \mathcal{S}_i := (\mathcal{D}_i \cup \mathcal{S}_i) \setminus (\mathcal{D}_i \cap \mathcal{S}_i)$ is given in Fig. 10. The width $\|\mathbf{w}\|$ of this set, as graphically defined in Fig. 10, is locally quadratic with $\|\mathbf{x}\|$. At least at one of the boundaries of $\mathcal{D}_i \Delta \mathcal{S}_i$, we know that $\mathbf{F}_i = \mathbf{F}_j$, due to continuity of the vector fields $\mathbf{F}$, where $j \in \{1, \ldots, \bar{m}\}$ is chosen such that $\mathcal{D}_j$ adjoins $\mathcal{D}_i$. Hence, we obtain $\|\mathbf{F}_j(\mathbf{x}, \nu) - \mathbf{F}_i(\mathbf{x}, \nu)\| = \mathcal{O}(L\|\mathbf{w}\|) = \mathcal{O}(L\|\mathbf{x}\|^2)$, where (1) and (2) both have a Lipschitz constant L. This implies:

$$\|\tilde{\mathbf{F}}_j(\mathbf{z}, \nu) - \tilde{\mathbf{F}}_i(\mathbf{z}, \nu)\| = \mathcal{O}(\nu^3 L c^2), \quad \forall \mathbf{z} \in (\tilde{\mathcal{D}}_i \Delta \mathcal{S}_i) \cap R(\nu), \tag{60}$$

where $\tilde{\mathcal{D}}_i \Delta \mathcal{S}_i := (\tilde{\mathcal{D}}_i \cup \mathcal{S}_i) \setminus (\tilde{\mathcal{D}}_i \cap \mathcal{S}_i)$.

Note that the state space can be partitioned as follows:

$$\mathbb{R}^2 = \bigcup_{i=1,\ldots,m} \left(\bar{\tilde{\mathcal{D}}}_i \cap \bar{\mathcal{S}}_i\right) \cup \bigcup_{i=1,\ldots,m} \left(\tilde{\mathcal{D}}_i \Delta \mathcal{S}_i\right).$$

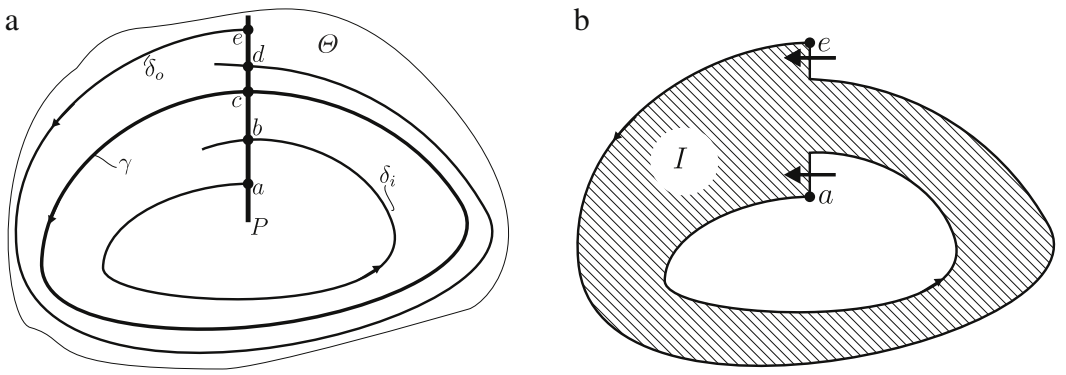

Fig. 11. (a) Stable limit cycle γ of (61) with two nearby trajectories and Poincaré section P. (b) Invariant set I of (62), depicted shaded, that is bounded by trajectories of (62) from points a and e.

This implies that combination of (59) and (60) yields $\|\tilde{\mathbf{F}}(\mathbf{z}, \nu) - \tilde{\mathbf{f}}(\mathbf{z})\| = \mathcal{O}(\nu^3 c^2, \nu^2 c, \nu, \nu^3 L c^2)$, $\forall \mathbf{z} \in R(\nu)$, such that for all $D > 0$ and bounded domain $R(\nu)$ defined in the Lemma, we can find a $\bar{\nu} \neq 0$ such that

$$\|\tilde{\mathbf{F}}(\mathbf{z}, \nu) - \tilde{\mathbf{f}}(\mathbf{z})\| \leq D, \quad \forall \nu \in (-\bar{\nu}, \bar{\nu}), \forall \mathbf{z} \in R(\nu). \quad \square$$

Lemma 17. *If the dynamical system*

$$\dot{\mathbf{z}} = \mathbf{f}(\mathbf{z}), \tag{61}$$

exhibits a stable or an unstable limit cycle, denoted $\gamma \in \Theta$, with $\mathbf{f} : \mathbb{R}^2 \to \mathbb{R}^2$ a Lipschitz continuous function and $\Theta \subset \mathbb{R}^2$ an open set containing no other limit sets, then there exists a $D > 0$ such that the dynamical system

$$\dot{\tilde{\mathbf{z}}} = \mathbf{f}(\tilde{\mathbf{z}}) + \mathbf{g}(\tilde{\mathbf{z}}), \tag{62}$$

has at least one closed orbit in Θ when $\|\mathbf{g}(\tilde{\mathbf{z}})\| \leq D$, $\forall \tilde{\mathbf{z}} \in \Theta$. When the Poincaré return map taken transversal to the closed orbits of (62) in Θ does not have non-isolated fixed points, then at least one of these orbits is a limit cycle with the same stability properties as γ.

Proof. Consider a line P that is locally transversal to the set γ of (61), as depicted in Fig. 11(a). Let the point c be the point of intersection of γ with P. First, we assume γ is asymptotically stable, such that there should exist trajectories $\delta_i \in \Theta$ and $\delta_o \in \Theta$ of (61) as depicted in Fig. 11(a), that are converging to the limit cycle and encircle the same equilibria. Notice that the intersection b of δ_i with P lies in the interior of $[a, c]$ and the intersection d of δ_o with P lies in the interior of $[c, e]$.

Now, we will determine a maximum difference $E > 0$ and time interval $[0, T + \tau_i]$, such that $\|\mathbf{z}(t) - \tilde{\mathbf{z}}(t)\| < E, \forall t \in [0, T+\tau_i]$ would imply similar behaviour for the trajectories of (61) and (62). Any such difference can be obtained by choosing D small enough, since both systems are Lipschitz continuous.

The following argument is similar as in the proof of Theorem 8. Let T be chosen such that $\mathbf{z}(T) = b$ when $\mathbf{z}(0) = a$. We choose a small $\tau_i > 0$ such that the trajectory $\mathbf{z}(t)$ from $\mathbf{z}(0) = a$ satisfies $\|\mathbf{z}(t) - b\| < \min(\|a - b\|, \|c - b\|), \forall t \in [T - \tau_i, T + \tau_i]$. When the trajectory $\mathbf{z}(t)$, $t \in [0, T + \tau_i]$ of (61) from $\mathbf{z}(0) = a$ and $\tilde{\mathbf{z}}(t)$, $t \in [0, T + \tau_i]$ of (62) from $\tilde{\mathbf{z}}(0) = a$ satisfy $\|\mathbf{z}(t) - \tilde{\mathbf{z}}(t)\| \leq E_i$, for $t \in [0, T + \tau_i]$, with $E_i > 0$ small enough, then the trajectory $\tilde{\mathbf{z}}(t)$ from $\tilde{\mathbf{z}}(0) = a$ traverses the interior of $[a, c]$ in a time interval $t \in (T - \tau_i, T + \tau_i)$.

In a similar fashion, we can derive τ_o and E_o, such that when the trajectory $\mathbf{z}(t)$, $t \in [0, T + \tau_o]$ of (61) from $\mathbf{z}(0) = b$ and $\tilde{\mathbf{z}}(t)$, $t \in [0, T + \tau_o]$ of (62) from $\tilde{\mathbf{z}}(0) = e$ satisfy $\|\mathbf{z}(t) - \tilde{\mathbf{z}}(t)\| \leq E_o$, $t \in [0, T + \tau_o]$, with $E_o > 0$ small enough, then the trajectory $\tilde{\mathbf{z}}(t)$ from $\tilde{\mathbf{z}}(0) = e$ traverses the interior of $[c, e]$ in a time interval $t \in (T - \tau_o, T + \tau_o)$.

Now, let $E = \min(E_i, E_o)$. When L is a Lipschitz constant of $\mathbf{f}(\mathbf{x})$, Theorem 3.4 of [17] implies $\|\mathbf{z}(t) - \tilde{\mathbf{z}}(t)\| \leq E$, $t \in [0, \max(T + \tau_i, T + \tau_o)]$ is satisfied for the trajectories from $\mathbf{z}(0) = \tilde{\mathbf{z}}(0) = a$ and $\mathbf{z}(0) = \tilde{\mathbf{z}}(0) = e$, when $E = \frac{D}{L}\left(\mathrm{e}^{L \max(T+\tau_i, T+\tau_o)} - 1\right)$, such that choosing a positive $D \leq \bar{D} := \frac{LE}{\mathrm{e}^{(L \max(T+\tau_i, T+\tau_o))} - 1}$ renders $E > 0$ small enough. In that case, the orbits of (61) and (62) from the point a both show, during one rotation, a diverging spiralling motion with respect to the origin. Similarly, the orbits of (61) and (62) from the point e show a converging spiralling motion during one rotation.

Since (61) is Lipschitz continuous, when a and e are chosen close enough to c and a positive $D \leq \bar{D}$ is chosen small enough, the function $\mathbf{n}_p^T \dot{\tilde{\mathbf{z}}}$ is of constant sign on the line segment $[a, e]$, where a normal vector $\mathbf{n}_p$ of P is introduced. This implies that the domain I is a positively invariant set, with I bounded by two trajectories of (62) and two line segments of $[a, e]$, as depicted in Fig. 11(b). In addition, the points a and e can be chosen such, that the domain I does not contain equilibria of (62) and all trajectories of (62) remain in Θ for $t \in [0, T + \tau]$. Therefore, the Poincaré–Bendixson theorem; see [10], guarantees the existence of a closed orbit in I for system (62).

Since I is a positively invariant set, a stable limit set of (62) exists in I. This follows from studying the return map of the perturbed system (62), which should be monotonous, to allow uniqueness of solutions in reverse time. Denoting the return

map of the perturbed system with $\tilde{M}$, we observe that $\|\tilde{M}(a)\| > \|a\|$ and $\|\tilde{M}(e)\| < \|e\|$. Since $\|a\| < \|e\|$, this implies that the monotonous function $x_{k+1} = \tilde{M}(x_k)$ has to cross the line $x_{k+1} = x_k$ from $\|\tilde{M}(x_k)\| > \|x_k\|$ towards $\|\tilde{M}(x_k)\| < \|x_k\|$ in the interval $x_k \in [a, e]$. When no non-isolated fixed points in this return map can occur, as stated in the lemma, then the perturbed system (62) exhibits a limit cycle which is asymptotically stable. The case of an unstable limit cycle follows analogously by studying the time-reversed systems. □

Using this Lemma, Theorem 11 can be proven. By Assumption 7, all closed orbits of (1) are limit cycles. At given system parameter ν, for each stable or unstable limit cycle γ_i, $i = 1, \ldots, l$, of system (1), we can define an open set $R_i(\nu) \ni \gamma_i$, containing no other limit sets. We apply the coordinate transformation $\mathbf{z} = \frac{\mathbf{x}}{|\nu|}$, relating (2) to (55) and (1) to (56), since we assumed $\mu = \nu$. Using Assumption 8, all limit cycles γ_i, $i = 1, \ldots, l$ of (1) are represented in the system (56), such that (56) contains the same number l of limit cycles, denoted $\bar{\gamma}_i$, $i = 1, \ldots l$, and the stability properties of γ_i and $\bar{\gamma}_i$ correspond for $i = 1, \ldots l$.

Combination of Assumption 7 and Lemma 17 yields that, since $R_i(\nu)$ is an open set and the system (1) is Lipschitz continuous, there exists a $D > 0$ such that when

$$\|\tilde{\mathbf{F}}(\mathbf{z}, \nu) - \tilde{\mathbf{f}}(\mathbf{z})\| \leq D, \quad \forall \mathbf{z} \in R_i(\nu), \tag{63}$$

holds, then k_i limit cycles of (55) exists in $R_i(\nu)$, of which at least one has the same stability properties as γ_i. According to Lemma 16, a neighbourhood N of $\nu = 0$ exists, such that condition (63) is satisfied. Applying the reversed transformation $\mathbf{x} = |\mu|\mathbf{z}$, we obtain k_i limit cycles of the conewise affine system (2), of which at least one has the same stability properties as γ_i.

The proof of the theorem is concluded by proving $k_i = 1$, $\forall i = 1, \ldots, l$, which is proven by contradiction. Suppose that there exists a domain $R_i(\nu)$ with $k_i \geq 2$ stable or unstable limit cycles $\gamma_{i,j}$, $j = 1, \ldots, k_i$, existing in the system (2) in the domain $R_i(\nu)$, $i = 1, \ldots, l$. For all these sets $\gamma_{i,j}$, $j = 1, \ldots, k_i$, we can find non-overlapping domains $R_{i,j}(\nu) \subset R_i(\nu)$, $j = 1, \ldots, k_i$, containing only one limit cycle. Using the same reasoning as above, we obtain that therefore, every set $R_{i,j}(\nu)$ contains a limit cycle of the nonsmooth system (1), implying $R_i(\nu)$ contains at least k_i limit cycles. By construction however, $R_i(\nu)$ contains only one such set, yielding a contradiction. Therefore, $k_i = 1$ for all $i \in \{1, \ldots, l\}$. Hence, the numbers of stable or unstable limit cycles of (1) and (2) are equal. In addition, their stability properties are equal. □

References

[1] R.I. Leine, H. Nijmeijer, Dynamics and bifurcation of non-smooth mechanical systems, in: Lecture Notes on Applied and Computational Mechanics, vol. 18, Springer-Verlag, Berlin, Heidelberg, 2004.
[2] D. Liberzon, Switching in Systems and Control, Systems and Control: Foundations & Applications, Birkhäuser, Boston, 2003.
[3] S. Coombes, Neuronal networks with gap junctions: A study of piecewise linear planar neuron models, SIAM Journal on Applied Dynamical Systems 7 (3) (2008) 1101–1129.
[4] H.J. Oberle, R. Rosendahl, Numerical computation of a singular-state subarc in an economic optimal control model, Optimal Control Applications & Methods 27 (4) (2006) 211–235.
[5] M. di Bernardo, C.J. Budd, A.R. Champneys, P. Kowalczyk, A.B. Nordmark, G.O. Tost, P.T. Piiroinen, Bifurcations in nonsmooth dynamical systems, SIAM Review 50 (4) (2008) 629–701.
[6] A.B. Nordmark, Non-periodic motion caused by grazing incidence in an impact oscillator, Journal of Sound and Vibration 145 (2) (1991) 279–297.
[7] R.I. Leine, Bifurcations of equilibria in non-smooth continuous systems, Physica D 223 (1) (2006) 121–137.
[8] M. di Bernardo, C.J. Budd, A.R. Champneys, P. Kowalczyk, Piecewise-smooth dynamical systems, in: Applied Mathematical Sciences, vol. 163, Springer-Verlag, London, 2008.
[9] R.I. Leine, D.H. van Campen, B.L. van de Vrande, Bifurcations in nonlinear discontinuous systems, Nonlinear Dynamics 23 (2) (2000) 105–164.
[10] P. Hartman, Ordinary differential equations, 2nd Edition, in: Classics in Applied Mathematics, vol. 38, SIAM, Philadelphia, 2002.
[11] T. Fujisawa, E.S. Kuh, Piecewise-linear theory of nonlinear networks, SIAM Journal on Applied Mathematics 22 (2) (1972) 307–328.
[12] M.K. Camlibel, W.P.M.H. Heemels, J.M. Schumacher, Algebraic necessary and sufficient conditions for the controllability of conewise linear systems, IEEE Transactions on Automatic Control 53 (3) (2008) 762–774.
[13] A. Arapostathis, M.E. Broucke, Stability and controllability of planar, conewise linear systems, Systems & Control Letters 56 (2) (2007) 150–158.
[14] E.A. Coddington, N. Levinson, Theory of ordinary differential equations, in: International Series in Pure and Applied Mathematics, McGraw-Hill Book Company, New York, 1955.
[15] M.W. Hirsch, S. Smale, Differential equations, dynamical systems and linear algebra, in: Pure and Applied Mathematics, vol. 60, Academic Press, London, 1974.
[16] M.S. Branicky, Multiple Lyapunov functions and other analysis tools for switched and hybrid systems, IEEE Transactions on Automatic Control 43 (4) (1998) 475–482.
[17] H.K. Khalil, Nonlinear Systems, 3rd ed., Prentice Hall, Upper Saddle River, 2002.
[18] A.A. Andronov, E.A. Leontovic, I.I. Gordon, A.G. Maier, Qualitative Theory of Second-order Dynamic Systems, John Wiley & Sons, New York, 1973.
[19] J.J.B. Biemond, Bifurcations in planar nonsmooth systems, Master's thesis, Eindhoven University of Technology, DCT internal report 2009.012 (2009).
[20] T.S. Parker, L.O. Chua, Practical Numerical Algorithms for Chaotic Systems, Springer-Verlag, New York, 1989.
[21] H. Nijmeijer, A. van der Schaft, Nonlinear Dynamical Control Systems, Springer-Verlag, New York, 1990.
[22] Yu.A. Kuznetsov, Elements of applied bifurcation theory, 2nd Edition, in: Applied Mathematical Sciences, Vol. 112, Springer-Verlag, New York, 1995.